UNIVERSITÀ DEGLI STUDI
DI NAPOLI FEDERICO II

Ahmed Adel M A Ibrahim Sallam

# BEC - Bridge Edge Curbs – GFRP rebar reinforcement

FRP++
Advanced structural analysis and design using composite materials

Master Dissertation
European Master Advanced Structural Analysis and Design using Composite Materials

Work developed under the supervision of
**Professor Marco Di Ludovico**
**Doctor Aniello Giamundo**
Co-Supervisors
**Doctor Andrea Miano**
**Doctor Annalisa Mele**

**Funded by the European Union**

(September) of (2023)

**DECLARATION**

**Name**: AHMED ADEL MOHAMED ABDELRAHIM IBRAHIM SALLAM

**Email:** SallamAhmed@myyahoo.com **Phone number:** (+39) 3761639246

**Title of the Master Thesis:** BEC - Bridge Edge Curbs – GFRP rebar reinforcement

**Supervisors:**

Prof. Marco Di Ludovico
Dr. Aniello Giamundo

**Co-Supervisors:**

Dr. Andrea Miano
Dr. Annalisa Mele

**Year of Conclusion**: 2023

Master Course in Advanced Structural Analysis and Design using Composite Materials



University of Naples Federico II, 08/09/2023

Signature:

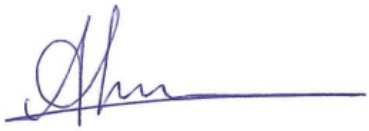

# ACKNOWLEDGEMENTS

I am incredibly grateful to have this opportunity to extend my heartfelt appreciation and gratitude to the following individuals, whose unwavering support, encouragement, and love have been instrumental in the completion of my Master of Science thesis.

My Father and Mother, you have been my pillars of strength throughout this journey and my entire life. Your unyielding belief in my potential, constant encouragement, and endless sacrifices have inspired me to reach new heights. Your love and guidance have been a constant source of motivation, and I am forever indebted to you both.

My Brother and Sister, your unwavering support and understanding have meant the world to me. You have always been there to lend a helping hand, provide valuable insights, and cheer me on during the most challenging times. I am truly grateful for having you as my siblings and as my friends.

My Fiancée, you are my rock, my confidant, and my biggest supporter. Your love and understanding have been an unwavering source of strength, helping me to stay focused and determined to complete this thesis. Your belief in my abilities and your willingness to stand by my side through every challenge mean the world to me.

My Friends, I am blessed to have such an incredible circle of friends who have been with me through thick and thin. Your presence, laughter, and camaraderie have made this academic journey enjoyable and meaningful. Thank you for your continuous encouragement and for being a constant source of joy in my life.

All my teachers and professors, I extend my heartfelt appreciation to all the educators, especially my supervisors, and co-supervisors who have played a pivotal role in shaping my academic growth. Your dedication to imparting knowledge, your guidance, and your commitment to nurturing our potential have been invaluable. You have instilled in me a passion for learning that will remain with me throughout my life.

Completing this MSc thesis would not have been possible without the collective support of these remarkable individuals. Each of you has contributed in your unique way to this accomplishment, and for that, I am forever grateful. Your faith in me has propelled me forward, even during moments of self-doubt.

I acknowledge that this achievement is not mine alone; it belongs to all of you as well. Thank you for being the pillars of my life and for accompanying me on this rewarding journey. Your love and support have touched my heart, and I look forward to sharing many more milestones with each one of you.

I would like to extend my heartfelt gratitude to ATP Company for their invaluable support and assistance throughout the course of my thesis work. Their generous provision of the essential materials, namely the GFRP rebars, was instrumental in the success of our experimental campaign and the completion of this research endeavour. ATP Company's unwavering commitment to fostering innovation and their dedication to advancing engineering solutions played a pivotal role in this project's accomplishments. I am truly appreciative of their support, which has not only enriched my academic journey but has also contributed to the broader realm of structural engineering.

With profound gratitude,

Ahmed A Sallam.

# BEC - Cordoli del bordo del ponte – Rinforzo dell'armatura GFRP

## RIASSUNTO

La funzionalità e la sicurezza delle infrastrutture di trasporto, in particolare dei ponti, sono cruciali per il benessere e lo sviluppo economico delle comunità. In Italia, numerosi ponti devono affrontare problemi di degrado, in particolare la corrosione delle armature in acciaio. La presente tesi di master focalizza l'attenzione su possibili interventi volti a superare le problematiche connesse alla corrosione nelle travi di bordo di ponti in c.a. (cordoli, di seguito denominati *Bridge Egde Curbs*, BEC), accelerata dagli agenti atmosferici e dai cloruri dei sali stradali. Per contrastare questo problema, si analizza l'efficacia di soluzioni basate sulla sostituzione delle armature in acciaio con armature in polimero rinforzato con fibra di vetro GFRP, note per la loro durabilità e resistenza alla corrosione. La leggerezza del GFRP facilita anche l'installazione. La validazione della soluzione richiede la caratterizzazione delle proprietà meccaniche delle armature in GFRP e la progettazione di una nuova tipología di cordolo, considerando dimensioni, peso della barriera e carichi. Il presente studio analizza le problematiche connesse alla validazione di tale soluzione e progettazione della stessa. Tale soluzione può fornire un significativo contributo alla mitigazione delle problematiche connesse al degrado nei ponti esistenti garantendo, inoltre, un incremento della la vita utile delle infrastrutture critiche e riducendo i costi di manutenzione delle stesse. Lo studio si pone l'obiettivo di impattare sulle future pratiche di progettazione e manutenzione dei ponti, promuovendo reti di trasporto sostenibili e resilienti per le generazioni a venire.

**PAROLE CHIAVE:** Mitigazione della corrosione; Rinforzo in GFRP; Ponti BEC; Infrastrutture; Sostenibilità; Durabilità; rinforzo.

# BEC - Bridge Edge Curbs – GFRP rebar reinforcement


## ABSTRACT

The serviceability and safety of transportation infrastructures, especially bridges, are crucial for the well-being and economic development of communities. In Italy, numerous aging bridges face degradation issues, particularly steel reinforcement corrosion. This master's thesis investigates corrosion in Bridge Edge Curbs (BEC), accelerated by atmospheric agents and chlorides from road salts. To combat this, the thesis investigates the effectiveness of internal steel rebars with GFRP-Glass Fiber Reinforced Polymer rebars, known for their durability and corrosion resistance. GFRP's lightweight also facilitates installation. Validating the solution requires characterizing GFRP rebars' mechanical properties and designing a new bridge edge curb, considering dimensions, barrier weight, and loads. The solution under investigation may strongly contributes to the corrosion mitigation of existing reinforced concrete bridges; it allows extending the service life of critical infrastructures, reducing maintenance costs, and ensuring commuter safety. Findings can impact future bridge design and maintenance practices, fostering sustainable and resilient transportation networks for generations to come.



**KEYWORDS:** Corrosion Mitigation; GFRP Reinforcement; BEC-Bridges; Infrastructures; Sustainability; Durability; reinforcement.

# TABLE OF CONTENTS

# LIST OF FIGURES

# LIST OF TABLES

# LIST OF ABBREVIATIONS AND SYMBOLS

## Abbreviations

| | |
|---|---|
| ACI | American Concrete Institute |
| CEN | European Committee for Standardization |
| FRP | Fiber Reinforced Polymer |
| GFRP | Glass Fiber Reinforced Polymer |
| CFRP | Carbon Fiber Reinforced Polymer |
| CNR | Advisory Committee on Technical Recommendations for Construction |
| ISO | International Organization for Standardization |
| ASTM | American Society for Testing and Materials |
| NTC | Norme Tecniche per le Costruzioni [Technical Standards for Buildings] |
| $CO_2$ | Carbon Dioxide |
| BEC | Bridge Edge Curb |
| NSM | Near Surface Mounted |
| UV | Ultraviolet |
| RC | Reinforced Concrete |
| RSC | Reinforced / Strengthened Concrete |
| CAC | Coral Aggregate Concrete |
| NAC | Normal Aggregate Concrete |
| ULS | Ultimate Limit State |
| SLS | Serviceability Limit State |

## Symbols

*Latin Upper-case Letter*

| | |
|---|---|
| $A_b$ | The Cross Sectional Area of The Bar |
| $E$ | Young's modulus of Elasticity |
| $E_A$ | Tensile Rigidity |
| $E_{cm}$ | Secant Modulus of Elasticity of Concrete |
| $F_{fu,p}$ | Recorded Ultimate Load |
| $F_{ult}$. | Ultimate Tensile Load |

| | |
|---|---|
| $M_{Rd}$ | Moment Resistance Capacity |
| $M_{cr}$ | Cracking Moment |
| $N$ | Number of Test Specimens |

*Latin Lower-case Letter*

| | |
|---|---|
| $l_p$ | The length of Specimen to be Tested |
| $l_a$ | The length of Anchorage |
| $d_b$ | The Bar Diameter |
| $d$ | Effective Depth |
| $d_s$ | Concrete Cover |
| $f_{fu,p}$ | Tensile Strength |
| $f_{ctm}$ | Mean value of axial tensile strength of concrete |
| $f_{ck}$ | Characteristic compressive cylinder strength of concrete at 28 days |
| $f_{cm}$ | Mean value of concrete cylinder compressive strength |
| $f_{cd}$ | Design value of concrete compressive strength |
| $f_{ftm}$ | The mean value of the tensile strength for GFRP reinforcement |
| $f_{ftd}$ | The design tensile strength of FRP reinforcement |
| $f_{ftk}$ | The characteristic tensile strength value of FRP reinforcement |

*Greek Letters*

| | |
|---|---|
| $\sigma$ | Tensile Strength |
| $\Phi$ | Bar Diameter |
| $\sigma_{ult.}$ | Ultimate Tensile Strength |
| $\varepsilon_{ult.}$ | Ultimate Tensile Strain |
| $\varepsilon_{cu}$ | Ultimate Concrete Compressive Strain |
| $\varepsilon_{fd}$ | Design Strain for FRP Reinforcement |
| $\varepsilon_{fk}$ | Characteristic Strain for FRP Reinforcement |
| $\varepsilon_{fu,p}$ | Ultimate strain of the Specimen Bar |

THIS PAGE WAS INTENTIONALLY LEFT BLANK

# 1. INTRODUCTION

Italy, known for its historical landmarks and beautiful bridges, has a vast network of transportation facilities that are essential for economic growth and societal connectivity. Bridges are vital components of transportation infrastructure, facilitating the smooth flow of goods and people across various regions.

Italy has a huge number of bridges in its road network, it has a presence of one bridge for each 2 km of road. The Italian infrastructure network of roads and bridges is one of the most complex in the world, due to the orography of the territory. Italy is strongly interested by seismic and hydrogeological hazards and, in addition, degradation is common on infrastructures approaching the end of their nominal life [1].

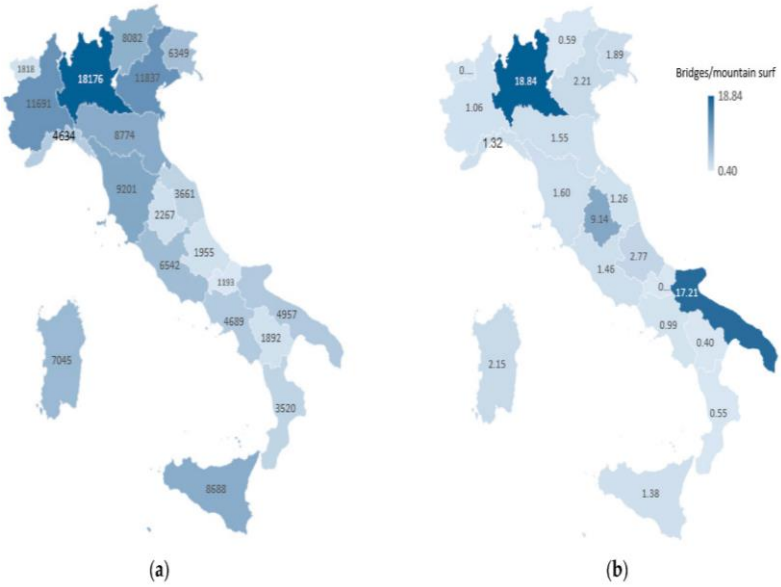


***Figure 1.1:*** *Distribution of Italian road bridges: (a) absolute number and (b) number of bridges per square kilometers of mountain surface [1].*

However, many of these bridges were built using traditional materials decades ago. The aging nature of many bridges, coupled with exposure to harsh environmental conditions, has led to corrosion and disintegration issues, especially in critical areas like the Bridge Edge Curb (BEC). The Bridge Edge Curb (BEC) is a crucial section of bridges that is particularly prone to corrosion due to its exposure to severe environmental components such as moisture, atmospheric agents, and chloride-laden de-icing solutions.

***Figure 1.2:*** *Explanation of the BEC - Bridge Edge Curb [2]*

The use of Composite materials, such as Glass Fiber Reinforced Polymer (GFRP), have gained significant attention and involved in various industries due to their unique properties and versatility. GFRP is a composite material composed of fine glass fibers embedded in a polymer matrix, usually epoxy resin. This combination provides exceptional mechanical properties to GFRP, making it lightweight, high-strength, corrosion-resistant, and durable. These attributes have led to its widespread adoption in the structural field and other engineering applications, revolutionizing traditional construction practices.

The use of GFRP reinforcement rebars in the structural field has seen remarkable growth due to their outstanding characteristics. Unlike steel reinforcement, GFRP rebars are not susceptible to corrosion, making them ideal for reinforcing concrete structures in harsh environments or marine applications. The lightweight nature of GFRP simplifies transportation and installation, reducing construction time and costs. Moreover, GFRP reinforcement rebars offer longer service life for structures, reducing the need for frequent maintenance. The adoption of GFRP reinforcement rebars in the structural field aligns with the industry's pursuit of sustainable and resilient infrastructure, creating safer and more durable constructions for the benefit of society.

## 1.1. Problem Statement

The BEC plays a pivotal role in supporting the bridge's load and providing a protective barrier for vehicular traffic. Material degradation pose significant challenges to the bridge's load capacity, barrier stability, and, ultimately, public safety.

The degradation and corrosion of Italian bridges, especially in the BEC region, have become pressing concerns for the government and transportation authorities. The aging infrastructure is exposed to corrosive environments, leading to the initiation and propagation of corrosion in steel reinforcement. This deterioration poses a serious threat to the structural integrity, safety, and serviceability of bridges, necessitating comprehensive corrosion mitigation strategies.

### *1.1.1. Degradation and Corrosion Challenges in BEC*

The BEC, located at the outer edge of the bridge deck, is continuously exposed to a range of environmental factors, including moisture, atmospheric agents, and chloride-laden salts used for de-icing during winter. Over time, these aggressive elements initiate and accelerate corrosion in the steel reinforcement of the BEC, causing deterioration and weakening of its structural integrity. The presence of cracks, spalling, and loss of cross-sectional area due to corrosion compromises the BEC's load-carrying capacity, raising concerns over the bridge's overall stability and safety.

### *1.1.2. Impact on load Capacity of Bridge*

Corrosion-induced degradation in the BEC can severely reduce the bridge's load-carrying capacity. The effective cross-sectional area of the steel reinforcement reduces as the corrosion continues, reducing its ability to resist loads and stresses. This loss of capacity can result in structural failures such as deflections, excessive deformations, and, in extreme circumstances, collapse. The lower load capacity endangers both the safety of bridge users and the structural integrity of the entire structure.

### *1.1.3. Barrier Stability and Vehicular Safety*

The BEC serves as a protective barrier for vehicular traffic, keeping cars from mistakenly deviating off the bridge deck in addition to bearing the bridge's load. Corrosion can degrade the structural integrity of the BEC, rendering it less efficient in guaranteeing the safety of vehicles and passengers. A weakened barrier increases the possibility of accidents and poses a major risk to public safety, particularly on high-traffic bridges.

### *1.1.4. Safety of Pedestrians and Cyclists*

The stability of the BEC is critical in ensuring the safety of walkers and cyclists on bridges with pedestrian walkways or dedicated bike pathways. The BEC's deterioration and corrosion can create dangerous situations for non-motorized users, exposing them to potential accidents and injury. It is critical to ensure the integrity and safety of the BEC in order to create a secure and user-friendly environment for all bridge users.

### *1.1.5. Mitigation and Preventive Measure*

Proactive actions are required to address the degradation and corrosion issues in the BEC. Regular inspections, maintenance, and repair are required to detect and address indicators of degradation as soon as possible. Furthermore, using advanced materials such as Glass Fiber Reinforced Polymer (GFRP) reinforcement can give a long-lasting and corrosion-resistant alternative, increasing the bridge's lifetime and safety.

In brief, the degradation and corrosion of Bridge Edge Curbs (BEC) are essential issues that have a direct impact on the bridge's load capacity, the stability of the barrier, and the safety of bridge users. To maintain the sustainability and safety of our critical transportation infrastructure, addressing these concerns demands, a holistic approach that includes timely maintenance, proactive inspections, and the use of new materials is needed. By preserving the integrity of BEC and bridges in general, we can continue to provide safe and efficient mobility for communities while also ensuring the public's safety.

## 1.2. Research Objectives

The primary objective of this master's thesis is to examine corrosion problems and degradation in Italian bridge BECs, as well as to validate a new solution to replace steel rebars by using GFRP reinforcing rebars (demolition of obsolete BEC and reconstruction with a new one is needed). The research objectives of the study are as follows:

1. Evaluate the extent and severity of corrosion in the BEC through detailed field assessments.
2. Define the environmental factors contributing to corrosion initiation and propagation in the BEC, considering climatic conditions, chloride exposure, and atmospheric agents.
3. Propose innovative corrosion mitigation strategies for the BEC region, with a particular focus on the application of advanced materials to enhance bridge durability.
4. Study the chosen material and characterize its mechanical behaviour, and its validity for the application.
5. Design, and certify the new design with the new material to be ready for application.

## 1.3. Significance of the Study

The findings of this study have substantial implications for bridge engineering and transportation infrastructure maintenance in Italy. Understanding the corrosion issues in the BEC can raise awareness among politicians and bridge authorities, emphasizing the importance of prompt bridge maintenance and repair. Furthermore, proposed corrosion mitigation technologies, such as the use of Glass Fiber Reinforced Polymer (GFRP) reinforcement, provide a viable alternative to improve bridge corrosion resistance and service life.

## 1.4. Thesis Outline

This master's thesis is structured into five chapters, each focusing on specific aspects of corrosion problems and degradation in Italian bridges, and the way of the application of the solution proposed. The outline of the thesis is as follows:

**Chapter 1: Introduction**

This chapter provides an overview of the corrosion and degradation problems faced by Italian bridges, outlining the significance of the study, research objectives, and the thesis's structure.

**Chapter 2: Defects in BEC-Bridge Edge Curbs & Reason to Use FRP**

The chapter focuses on the following aspects:

- Statistical analysis of the common defects observed in BEC of bridges.
- Examination of the factors contributing to degradation and corrosion in this critical area.
- Identification of the most prevalent issues and their impact on the overall structural integrity.

**Chapter 3: Experimental Campaign: Mechanical Characterization of GFRP Rebars**

The chapter focuses on the following aspects:

- Review of the current state of art on the use of Fiber Reinforced Polymer (FRP) in structural applications.
- Analysis of GFRP's unique properties.
- Properties experimental characterization tests adhering to relevant codes.
- Experimental Campaign.

**Chapter 4: Design and Verifications of Bridge Edge Curb with GFRP rebars**

The chapter focuses on the following aspects:

- Development of a design procedure for BEC using GFRP reinforcement rebars as an alternative to traditional steel rebars.
- Calculations of the minimum reinforcements needed in the case of BEC using GFRP reinforcement rebars.
- Validation of the structural integrity and safety of the new BEC through extreme events such as a vehicle smash against the barrier.

**Chapter 5: Conclusions and Future Scope**

This chapter provides a summary of the research findings and their implications for corrosion mitigation in BEC, discusses the effectiveness and benefits of using GFRP reinforcement rebars, and finally, remarks on the significance of this study and its contribution to bridge engineering and corrosion mitigation.

# 2. DEFECTS IN BEC-BRIDGE EDGE CURBS AND REASON TO USE FRP

A comprehensive statistical analysis of the defects observed in Bridge Edge Curbs (BEC) based on inspection data collected from a large number of bridges. The examination of this extensive dataset allows us to identify common degradation and corrosion issues prevalent in the BEC region. By analysing the frequency and severity of these defects, we gain valuable insights into the factors contributing to the deterioration of this critical area in Italian bridges. The statistical findings form a foundational basis for understanding the scope of the problem and serve as a crucial starting point for our subsequent investigations into effective corrosion mitigation strategies using Glass Fiber Reinforced Polymer (GFRP) reinforcement rebars.
An Italian defects catalogue [3] has been used to collect the description, causes, and example photos of the defects.

In order to work on modifying the BEC-Bridge Edge Curbs by replacing the steel reinforcement rebars with GFRP rebars, we should to know at first the nature, and the causes of the defects occur in this particular part to find the best solutions to avoid it.

The objective is to figure out the most common defects occur in the BEC-Bridge Edge Curbs, and its effect as follows:

1- Filtering the BEC defects from some bridges' defects inspection reports.
2- Defects description and causes.
3- The repetition of each defect.

## 2.1. BEC-Bridge Edge Curb

Viaduct edge elements are distinctly marked by the presence of road barriers that are strategically affixed onto specialized edge-bridge curbs. These curbs play a crucial role in delineating the boundary of the viaduct while also serving as a support structure for the road barriers. This configuration ensures the safety and containment of vehicles traveling on the viaduct, preventing any accidental veering off the road. The integration of road barriers onto these specialized curbs not only enhances traffic safety but also contributes to the overall stability and functionality of the viaduct structure.

***Figure 2.1:*** *Identification of the edge-bridge curb [4]*

In case of extraordinary maintenance interventions, such as:

- installation of new safety barriers, noise barriers or integrated;
- widening of the roadway;
- replacement of existing barriers;

it is frequently necessary the intervention of partial or total reconstruction of the curb.

In cases where the renovation or adjustment of a curb edge-bridge must be performed in an emergency or you want to limit the arc as much as possible intervention time on the road platform the choice to make a curb in fiber-reinforced concrete can be optimal.

The use of concrete with added dispersed steel fibers instead of steel reinforcing bars, saves the time needed to assemble the cage before pouring the concrete and reduces enormously the fixing time of the barrier above the curb. The latter saving is linked to two fundamental aspects: the lack of reinforcing bars allows operators to drill the curb easier and faster for insert the anchor bolts of the barrier uprights and the rapid hardening of this type of blends allows you to work on the element already after a couple of days from the casting of the curb.[4]

The analysis section is limited to only curb, regardless of the other elements to which it is connected, as well as identified in the following **Figure 2.2**.

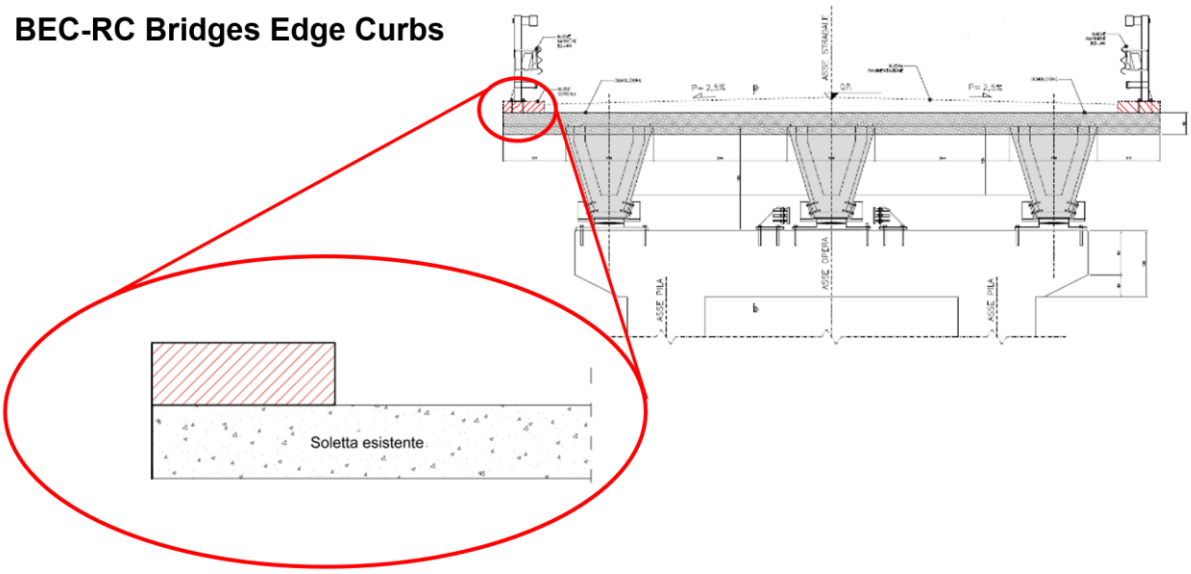


***Figure 2.2:*** *Identification of the local intervention section highlighted with red hatching lines.*

## 2.2. The BEC Defects

The most common defects occurring in the BEC are illustrated in the following,

### *2.2.1. ORDINARY REINFORCEMENT UNCOVERED/OXIDIZED*

**DESCRIPTION**

The "uncovering" of the reinforcement indicates the lack of covering concrete and therefore often appears combined with the concrete defects; oxidation of the armor typically begins to occur when the same is still inside the concrete cover (cf. carbonation phenomenon, etch from chlorides, etc.) and it will remain exposed after the mechanical expulsion of the concrete cover afterwards of the expansion. Once exposed, the armor will be subject to a speed increase of degradation.

**CAUSE**

The lack of covering is caused by the deterioration of the concrete (detachment or washout) or by errors in the execution phase (crawl spaces or lack of concrete cover) or by accidental causes (vehicle collisions).

***Figure 2.3:*** *Example Photos of ORDINARY Reinforcement UNCOVERED/OXIDIZED Defect*

### *2.2.2. DETERIORATED SUBSEQUENT FILMING*

**DESCRIPTION**

By " subsequent shooting " we mean repairs locate carried out on the concrete; usually, it is the filling of voids, the clogging of crawl spaces or the reconstruction of the concrete cover or of the edges detached; on these areas can stand out all anomalies _ typical of concrete which washout, deterioration and injury miscellaneous and in addition the detachment or injuries between the material old and the new. All these anomalies are briefly and exclusively described by the defect in question.

**CAUSE**

The main causes that generate these anomalies: – the use of inappropriate materials; – poor execution of the repair (e.g., cavities filled only superficially or inadequate preparation of the attachment surfaces); – the set of external agents that commonly attack structures (e.g., freeze/thaw, carbonation, etc.).

***Figure 2.4:*** *Example Photos of DETERIORATED SUBSEQUENT FILMING Defect*

### *2.2.3. REDUCTION OF RESISTANT SECTION OF THE CONCRETE*

**DESCRIPTION**

It's a flaw detectable on all concrete structures, but here the focus is on those elements such as: piers and abutments, arches in reinforced concrete and cap, beams in cap in which the section is considered entirely reagent. It is usually accompanied by the defects of the armor, both slow and prestressing.

**CAUSE**

The reduction of the reacting section, apart from that due to accidental events (e.g., impacts) generally corresponds to an advanced state of deterioration of the concrete, due to progressive oxidation and corrosion of the reinforcements, expansion with disintegration of the surrounding concrete, increase of the surface exposed to the actions of degradation, repetition of the cycle of degradation on the parts that have remained exposed.

***Figure 2.5:*** *Example Photos of REDUCTION OF RESISTANT SECTION OF THE CONCRETE Defect*

### *2.2.4. CRAWL SPACES*

**DESCRIPTION**

Presence of humidity that has penetrated due to infiltrations or capillary rising through the concrete. It occurs more frequently on the intrados of the slabs (girder decks, caissons or slabs), but also through the vertical walls of the abutments (infiltration from the ground behind) or hollow piles (stagnant water inside).

**CAUSE**

It is a defect due to problems in the execution phase: separation of the aggregates, bad vibration, casting restarts or incorrect granulometric curve (mix design).

***Figure 2.6:*** *Example Photos of CRAWL SPACES Defect*

### *2.2.5. DISTURBED CONCRETE*

**DESCRIPTION**

The definition indicates different deterioration phenomena that appear together or individually on the concrete surface. Generally, the term "deterioration" refers to phenomena such as flaking, porosity, loss of cohesion, real or apparent swelling, etc. It is sometimes accompanied by cracking and almost always by defects in the underlying reinforcements.

**CAUSE**

The deterioration of the concrete, often exalted by the presence of a humid environment, is due to phenomena of a chemical nature (carbonation or attack of chlorides, which in reality do not act directly on the concrete but allow the oxidation process of the reinforcements to begin, the expansion generates localized disintegration of the material) or physical (freeze and thaw cycles) which are also linked to the climatic characteristics of the site. The entity of these phenomena is inversely proportional to the good execution of the concrete.

***Figure 2.7:*** *Example Photos of DISTURBED CONCRETE Defect*

### *2.2.6. MOISTURE STAINS*

**DESCRIPTION**

Presence of humidity that has penetrated due to infiltrations or capillary rising through the concrete. It occurs most frequently at the intrados of the slabs (girder decks, caissons or slabs), but also through walls verticals of the shoulders (infiltration from the ground behind) or hollow stacks (stagnant water inside).

**CAUSE**

In addition to the porosity of the material, the following are the contributing causes:

- Missing or insufficient waterproofing at the extrados of the slabs.
- The irregularities of the waste disposal or drainage systems waters.

***Figure 2.8:*** *Example Photos of MOSITURE STAINS Defect*

### *2.2.7. DRAINAGE TRACES*

**DESCRIPTION**

Defect generated by the repeated passage of water on the surface of the element concerned, made visible, when the water is not present, by the effects of the chemical action of the salts dissolved in it. It is a defect that can be found in all structures and on all materials; it is typical of vertical walls, but it is also detectable in horizontal structures, such as the overhangs of the slab, when the water coming from the crowning stagnates on their intrados.

**CAUSE**

All those that allow the passage of water as failure of imperfect waterproofing, irregularities of the water disposal, the imperfect joint tightness, and other related to details executives such as the absence of drips.

***Figure 2.9:*** *Example Photos of DRAINAGE TRACES Defect*

### *2.2.8. BRANCHED LESIONS AND DEGRADED CONCRETE*

**DESCRIPTION**

The defect appears as a set of lesions of various sizes with an irregular appearance, usually not in correspondence with the underlying frameworks. The surface of the structural element affected by this state of cracking does not resonate when struck with a hammer. Sometimes, a kind of gel is present on the flaps of the lesions. In an advanced state of deterioration, the concrete surface is deteriorated, with swelling and expulsion/detachment of the aggregates.

**CAUSE**

It is generally due to the chemical reaction between the alkalis (sodium and potassium) and some types of reactive aggregates (e.g., amorphous silica) present in the cement. This reaction produces a gelatinous substance capable of increasing in volume in a humid environment, causing localized swelling, cracking phenomena and concrete detachments.

***Figure 2.10:*** *Example Photos of BRANCHED LESIONS AND DEGRADED CONCRETE Defect*

### *2.2.9. REDUCTION OF REINFORCEMENT BARS SECTION*

**DESCRIPTION**

When the oxidation of the reinforcing rods of the reinforced concrete structures exceeds the surface layer, we can talk about a reduction in the section of the bars. Obviously, this defect must also be reported in the breakage of the bars, representing the last stage of section reduction. The flaw is always accompanied by degradation of the concrete.

**CAUSE**

The processes of degradation of the reinforcements are linked to design shortcomings (with regard to the systems of waterproofing, collection and water disposal) and executive (lack of concrete covers, crawl spaces, etc.); these processes have the extreme consequences over time, following the uncovering of the bars and in the presence of constant humidity, the reduction of the diameter of the bars. In other cases, the breakage of the armor is caused by shocks accidental.

***Figure 2.11:*** *Example Photos of REDUCTION OF REINFORCEMENT BARS SECTION Defect*

### *2.2.10. WASHED OUT CONCRETE*

**DESCRIPTION**

Removal of material, on a very reduced thickness, from the surface of the structure following the chemical/mechanical action carried out on it by running water. It is typical of elements such as abutments, piles, beams, cantilevers, slabs, etc. directly affected by the repeated passage of water (e.g., from unequipped expansion joints).

**CAUSE**

The phenomenon is favored by the action and/or aggressiveness of the waters (CO2 content) which percolate on surfaces; it is also related to the execution quality of the concrete. Especially if the water is aggressive, in contact with the cementitious matrix it generates the washout of the free lime and consequent degradation of the material, the removal of which is then due to the mechanical action.

***Figure 2.12:*** *Example Photos of WASHED-OUT CONCRETE Defect*

### *2.2.11. OXIDATION*

**DESCRIPTION**

Steel (particularly iron) reacts with the oxygen in the air in the presence of humidity, with the formation of oxide. It can occur in various stages of evolution: punctiform oxidation with perforation of the protective coating, slight surface degradation, swelling of the external surface, reduction in thickness (less than 5%). It concerns the metal structures and the steel arts of bearings and joints.

**CAUSE**

derives from missing or unsuitable preparation of the metal surfaces or from the lack or deterioration (e.g., due to lack of maintenance or impacts) of the protective paint. In such situations the presence of humidity is a contributing cause. Other causes may be the presence of stray currents or aggression by chlorides (antifreeze salts, marine environment, etc.).

***Figure 2.13:*** *Example Photos of OXIDATION Defect*

### *2.2.12. CONCRETE CORNER DETACHMENT*

**DESCRIPTION**

Detectable on all concrete structures; the corner area is in fact more exposed due to its high surface/volume ratio and therefore more subject to detachments. It is usually accompanied by defects in the reinforcement (especially the ordinary or subsidiary one, more rarely the prestressing ones), which the fall of the edge exposes.

**CAUSE**

It derives from the expansion due to the oxidation of the metal reinforcements and the thrust generated by the consequent swelling; can be due to accidental causes (bumps).

***Figure 2.14:*** *Example Photos of Concrete corner DETACHMENT Defect*

### *2.2.13. INFILTRATIONS DUE TO LACK OF SEALING RAINWATER INLET*

**DESCRIPTION**

When the efficiency of the sealing between the opening on the structure (slab, etc.) and the entrance to the downpipe, part of the water infiltrates and is dispersed at the intrados of the slab, instead to be correctly conveyed in the descendant.

**CAUSE**

Incorrect execution of sealing or progressive deterioration due to vibration or wear in type.

***Figure 2.15:*** *Example Photos of INFILTRATIONS DUE TO LACK OF SEALING RAINWATER INLET Defect*

### *2.2.14. CORROSION*

**DESCRIPTION**

Refers to the chemical process of oxidation of a steel element when it reaches a appreciable reduction (greater than 5%) of the thickness of the metal. It can be presented in different stages of evolution: from the slight reduction in thickness (in any case higher than 5%), to significant reduction from a structural point of view, up to the perforation of the metal. Regard metal structures and steel parts of supports and joints.

**CAUSE**

Derives from failure or unsuitability surface preparation metallic or by the lack or deterioration (e.g., due to the absence of maintenance or shocks) of the protective varnish. In such situations are caused by the presence of humidity and the non-timeliness of the maintenance interventions. Other causes may be the presence of currents wandering, aggression by chlorides (antifreeze salts, marine environment, etc.).

***Figure 2.16:*** *Example Photos of CORROSION Defect*

### *2.2.15. ABSENT OR PERMEABLE SEAL ELEMENT*

**DESCRIPTION**

This defines the presence of a percolation from the joint due to deterioration of the sealing element, or the lack of the element itself.

**CAUSE**

The sealing element may be missing from the start or later of the instability of the same, especially if of the type glued or pushed to pressure between the insoles; fall or break can be due to the wear of the constituent material or to the thrust of debris accumulated; another cause is the abnormal movements of the joints.

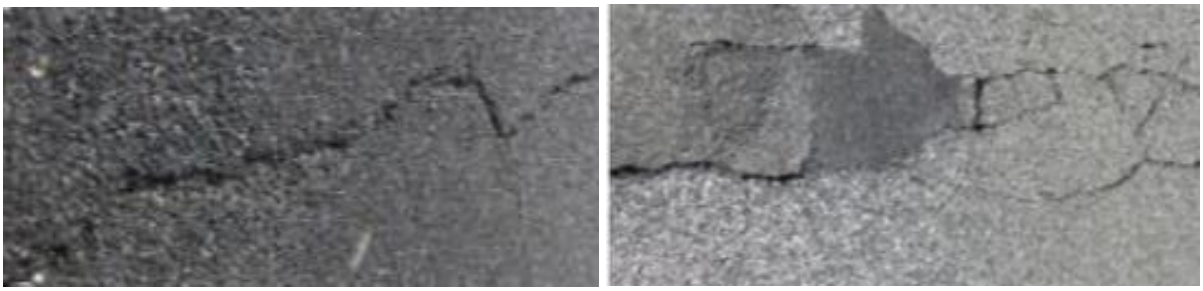

***Figure 2.17:*** *Example Photos of ABSENT OR PERMEABLE SEAL ELEMENT Defect*

## 2.3. Statistical Findings

According to the results of the performed statistical analysis of inspection data obtained from a large number of bridges, the "**ORDINARY Reinforcement UNCOVERED/OXIDIZED**" and "**Disturbed Concrete**" are the most common defects in the BEC-Bridge Edge Curb, where the corrosion in the steel reinforcement rebars is one of the main causes of their occurrence.

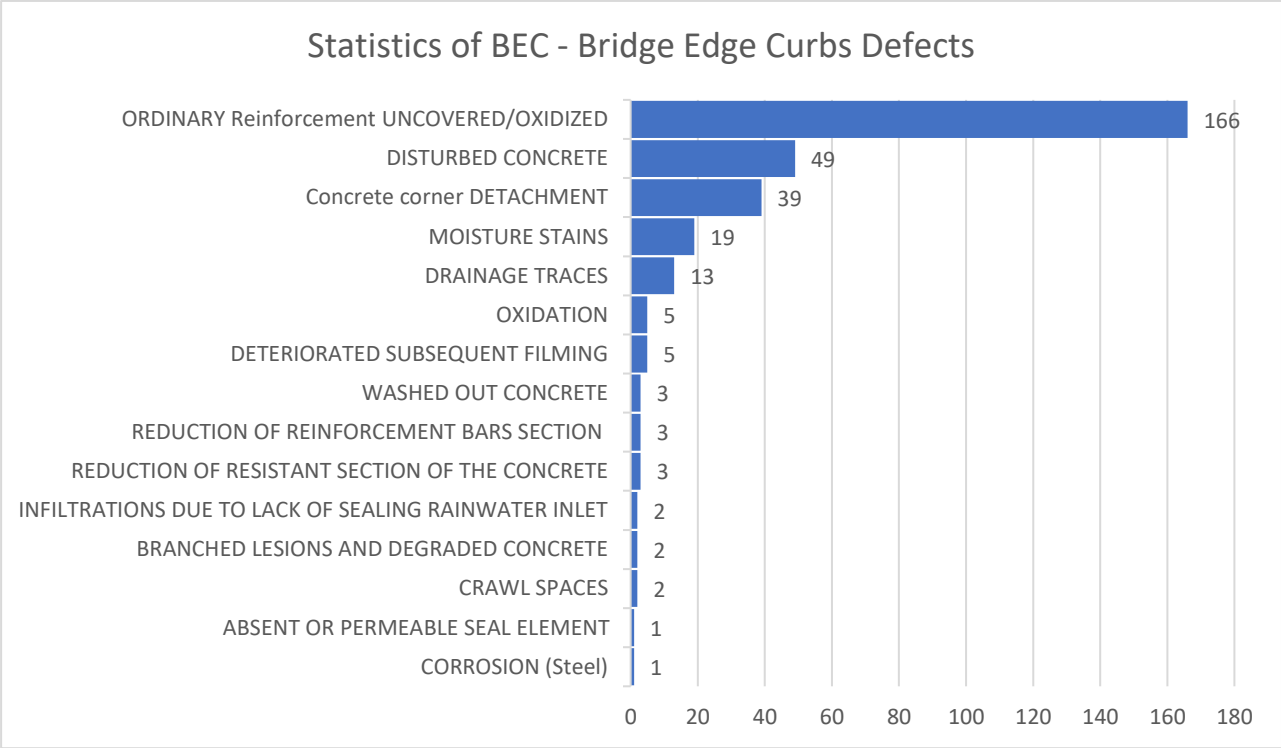


***Figure 2.18:*** *Frequencies of BEC-Bridge Edge Curb defect types*

In conclusion, Corrosion in the steel reinforcement rebars emerges as a major contributing factor to the occurrence of these defects. Based on this statistical evidence, the utilization of Glass Fiber Reinforced Polymer (GFRP) rebars clearly presents itself as a viable solution for addressing the majority of these defects. The corrosion-resistant nature of GFRP makes it an ideal alternative to steel, providing the potential to mitigate degradation and ensure the longevity and safety of critical bridge components.

# 3. Experimental Campaign: Mechanical Characterization of GFRP Rebars

The experimental campaign of GFRP rebars forms a pivotal chapter in this thesis, focusing on the comprehensive testing and characterization of Glass Fiber Reinforced Polymer (GFRP) reinforcement rebars. After a state of the art on the use of FRP in structural applications, this chapter aims to explore and evaluate the mechanical properties and performance of GFRP rebars through experimental tests. The findings of this experimental campaign will play a crucial role in validating the feasibility and effectiveness of using GFRP rebars as an alternative to traditional steel reinforcement rebars in critical structural applications, ultimately contributing to the advancement of sustainable and resilient construction practices.

## 3.1. State of Art on The Use of FRP in Structural Applications

The state of the art in the utilization of Glass Fiber Reinforced Polymer (GFRP) in the structural field embodies a transformative shift in modern engineering practices. GFRP, characterized by its exceptional mechanical properties and resistance to corrosion, has emerged as a versatile and promising material for enhancing the durability, sustainability, and performance of various structural components. The integration of GFRP within diverse sectors such as civil engineering, aerospace, maritime, and automotive industries reflect an innovative approach that addresses the challenges posed by traditional materials. This dynamic field showcases a rich tapestry of research endeavours, encompassing material characterization, design methodologies, and applications that highlight the profound impact of GFRP on reshaping the landscape of structural engineering.

A previous study about “Glass fibre reinforced plastic (GFRP) rebars for concrete structures” back in 1995 which was a part of a larger experimental and theoretical program on the application of FRP reinforcement for concrete structures, initiated at the department of civil engineering Université de Sherbrooke in Canada [5]. The study focuses on the flexural behaviour of concrete beams reinforced with GFRP rebars. It presents the properties of GFRP and its components, as well as an overview of relevant research activities involving GFRP

rebars as reinforcement for concrete units. The study discusses the influence of the volume and orientation of fibers on the creep behaviour of GFRP rebars, with additional strains caused by creep reported to be around 3% of the initial elastic strains. The use of high-strength concrete (69 MPa) instead of normal strength concrete (27.6 MPa) is beneficial to take advantage of the high tensile strength of GFRP rebars. The experimental results show that GFRP tension reinforcement behaves similarly to a tension test, indicating a perfect bond between the rebar and concrete.

A "Relevant Field Applications of FRP Composites in Concrete Structures" study was performed in 2001 by Center for Infrastructure Engineering Studies, University of Missouri, USA [6]. The study reports on nine relevant applications of FRP composites in concrete structures in the United States, including strengthening of concrete members with externally bonded FRP laminates or near surface mounted (NSM) bars. FRP materials have been used in small projects and some multi-million-dollar projects for strengthening parking garages, multi-purpose convention centers, office buildings, bridges, and silos. The American Concrete Institute (ACI) has published a design guide for internal FRP reinforcement and is expected to publish one on external FRP reinforcement, which will further expedite the adoption of composites in construction. The study also presents four field projects that used FRP bars as internal reinforcement for improved durability, including a concrete box culvert bridge reinforced with GFRP bars and the upgrade of a retail building to house a telecom hotel.
In conclusion, strengthening of concrete structures with externally bonded FRP laminates or NSM bars has gained significant market share, with several multi-million-dollar projects in the United States. The availability of design and construction guidelines for FRP technology will increase confidence and facilitate its widespread use in the industry.

A state-of-the-art review of fiber-reinforced polymer composites for construction applications in civil engineering has been provided by American society of civil engineers in 2002 [7], covering various aspects such as structural shapes, bridge decks, internal reinforcements, externally bonded reinforcements, and standards and codes. The authors provide a historical review, current state of the art, and future challenges for each section, indicating that the data used in the study includes past research, current advancements, and potential areas of improvement in the field of FRP composites for construction. The review also mentions the

use of FRP materials in primary load-bearing systems for general construction, as well as their applications in concrete structures for improved corrosion resistance and seismic retrofitting. Additionally, the review highlights the development, state of the art, and future directions of FRP composites, indicating that the data used includes research and demonstration projects funded by industries and governments around the world.

A review on FRP composites applications and durability concerns in the construction sector was held by Department of Civil Engineering, Faculty of Engineering-Rabigh, King Abdulaziz University, Kingdom of Saudi Arabia, and Department of Civil Engineering, Faculty of Engineering, Aswan University, Egypt[8]. The review stated that FRP composites offer numerous advantages over conventional building materials, such as lightness, high mechanical performance, and ease of installation, making them suitable for a wide range of applications in the construction industry. However, FRPs are also faced with challenges, including the lack of design codes, brittle behaviour of the fibers, anisotropic behaviour, and susceptibility to environmental conditions. Durability is a major concern for the widespread applicability of FRPs in the construction industry, as they can be affected by factors such as temperature, humidity, and the combined action of these factors. The durability of FRPs is influenced by both the matrix and the fiber, with the fibers contributing to their strength in tension. Overall, FRP composites offer interesting applications in the construction industry, but their acceptability and applicability are still subject to further investigation and improvement.

Another study provides a state-of-the-art review of the application and design of FRP reinforcement for concrete structures in 2014 [9]. It discusses the use of FRP composites in both new construction and the strengthening or repairing of existing buildings. The review highlights the need for standardization in the shape of FRP bars and anchoring measures for external reinforcement, which would allow for a more extensive use of FRP reinforcement in the construction industry. The study emphasizes the importance of considering long-term degradation of mechanical properties when designing FRP RC elements. It also identifies the absence of design codes, significant variation in the material properties of FRP composites, and limited knowledge among engineers as factors limiting the application of FRPs in building industry. The review identifies problematic issues related to the material properties of FRP

that are important for designing RC and formulates targets for further research in areas such as the long-term mechanical processes in concrete elements with FRP reinforcement and the development of design codes for FRP reinforcement.

International Institute for Urban Systems Engineering, Southeast University, China, in 2014 published State-of-the-art review of FRP composites for major construction with high performance and longevity [10]. The study reviews the state-of-the-art research of FRP in structural retrofitting and strengthening, identifying the challenges facing further development of FRP in civil engineering. Hong Kong has also conducted research in this field, with projects and guidelines that have solved many problems related to FRP reinforcement and promoted its application in civil engineering. There is a critical need for prolonging the service, safety, and durability of major structures, as traditional design methods often neglect the time variability of structural resistance and lack durability failure criteria and design methods. The fracture mechanism and size effect of FRP large structures need to be studied more thoroughly, and valuable lessons can be learned from the design of aircraft. Existing design methods may underestimate FRP brittle fracture or be too conservative, resulting in a waste in the use of these materials. A new model has been presented to predict the stress-strain response of FRP-confined concrete with high accuracy. In conclusion, FRP composites have broad application prospects for major constructions, but there are several bottlenecks that need to be resolved. Research and engineering applications of FRP reinforced structures have laid the necessary foundation for the use of high performance FRP and longevity of major structures. However, there are still challenges to be addressed, such as the study of failure mechanisms, durability performance, and life cycle design theory of large-scale FRP reinforced structures, especially under extreme loads and environmental conditions. The ongoing project described in the study aims to enhance the use of large-scale FRP component model tests and develop advanced numerical simulation tools to clarify size effects and damage evolution under extreme loads. The study also aims to establish a reliable short-term accelerated durability test method for FRP reinforced structures and form the basis for the reliability design of FRP reinforced large-scale structures.

A review on properties and applications of FRP in strengthening RC structures published in 2018 [11] that provides a comprehensive insight into the integrated applications of Fiber Reinforced Polymer (FRP) composite materials for improving the techniques of rehabilitation, repair, strengthening, and retrofit of concrete structures in the construction industry today. It reviews the design, matrix, material properties, applications, and serviceability performance of FRP. The study also discusses the strength-to-weight ratio, rigidity, electrical and thermal conductivity, and fatigue, corrosion, and fire resistance of FRP. It highlights the importance of using FRP to strengthen existing reinforced concrete (RC) structures and repair any deterioration, with the aim of developing a system that can resist natural disasters such as earthquakes, strong storms, and floods. The study highlights the importance of considering factors such as creep rupture reduction, thickness of FRP layer, and compressive strength of the strengthened concrete element zone when using FRP systems. FRP-concrete hybrid sections have been used in various projects since 1987, and this review aims to provide an in-depth review on their mechanical behaviours and properties for bridge applications.

A review on FRP-concrete hybrid sections for bridge applications in 2020 [12] was published which reviews the materials, sectional configurations, FRP-concrete shear connection, failure modes, deformation, and field applications of FRP-concrete hybrid sections. The review concludes that different types of fibers and manufacturing techniques of FRP have been developed, shear connections play a pivotal role in the structural performance, mathematical models need improvement to accurately predict failure modes, and effective measures are needed to improve the flexural stiffness. The study also emphasizes the need for more pilot bridge projects to understand the viability and features of FRP-concrete hybrid sections in bridge applications. The review provides case studies and discusses future development perspectives.

School of Highway, Chang ‘an University, China published a Review of Experimental Studies on Application of FRP for Strengthening of Bridge Structures in 2020 [13]. It reviews the development and applications of FRP materials for the strengthening and rehabilitation of bridge structures. It summarizes the types and properties of FRP composites and discusses the applications and development of FRP sheets, FRP bars, FRP grids, and prestressed FRP tendons for bridge structures. The study covers the FRP strengthening methods and the response

properties of flexural performance, bonding performance, and ductility. It presents significant conclusions regarding the strengthening/repair of bridge structures with FRP composites. The study details the current state of knowledge and research on strengthening bridge structures with FRP composites and is helpful for better understanding and establishing design criteria.

In 2021, a state-of-the-art review of coral aggregate concrete (CAC) and its combination with fiber-reinforced polymer (FRP) in marine engineering applications [14]. It discusses the physical properties of coral aggregates, including their porous structure and low strength characteristics. The mechanical properties of CAC under uniaxial and multiaxial compression are examined, highlighting its unique characteristics compared to ordinary concrete. The durability of CAC, particularly its chloride ion resistance and performance under drying-wetting cycles, is explored. The study also reviews the latest studies on the combination of FRP and CAC, including the use of FRP tubes and bars. Additionally, the characteristics of coral aggregates, such as their low strength, high deformability, and presence of chloride ions, are discussed. The bond-slip behaviour between FRP bars and concrete is examined, considering factors such as surface treatment methods and failure modes. The high porosity and water absorption behaviour of coral aggregates are also addressed, recommending prewetting before mixing concrete.

In conclusion, Coral aggregate concrete (CAC) is an economical and eco-friendly construction material that utilizes local raw materials on remote islands. It exhibits unique characteristics compared to ordinary concrete due to the porous structure and low strength of coral aggregates. The high porosity of coral aggregates contributes to the crushability and low strength of CAC, while the rough surface and high-water absorption contribute to the dense internal transition zone inside CAC. These characteristics have a profound impact on the properties of CAC. The early strength growth of CAC is fast due to the presence of chloride ions, but its long-term strength is lower than that of normal aggregate concrete (NAC). However, the tensile performance of CAC is similar to or better than that of NAC. Fiber-reinforced polymer (FRP) has been identified as a promising material for CAC construction to overcome the challenges of steel corrosion in marine environments. The combination of FRP and CAC, including the use of FRP tubes and bars, shows potential for further strength improvement.

A state of art review on Seismic upgrading of existing reinforced concrete buildings in 2021 [15] provides a review of seismic upgrading techniques for reinforced concrete (RC) buildings, focusing on both traditional and novel methods. The retrofitting methods are divided into two categories: local measures that enhance the behaviour of individual elements, and global measures that operate on the structure as a whole. Hybrid methods, such as the combination of FRP/TRM jackets with NSM strips, have been commonly used for flexural and shear strengthening of RC buildings. Seismic retrofitting techniques can be divided into conventional and novel ones, depending on their age and materials employed. Full CFRP wrapping and strap CFRP wrapping have been compared for external reinforcement in shear-controlled RC columns, with different studies showing varying results. The review concludes by discussing the strengths and weaknesses of both local and global retrofitting techniques, including the use of FRP and TRM materials.

Recently in 2023 an FRP-Reinforced/Strengthened Concrete: State-of-the-Art Review on Durability and Mechanical Effects was published [16]. A state-of-the-art review was provided on the key environmental and mechanical conditions affecting the durability and mechanical properties of FRP composites used in reinforced concrete structures. The study aims to help in the proper use of FRP materials for concrete structures by understanding their behaviour and effects on enhancing long-term performance. The most commonly used FRP composites for internal and external applications are Glass/vinyl-ester FRP bars and Carbon/epoxy FRP fabrics, respectively. The study highlights the key environmental and mechanical conditions that affect the durability and mechanical properties of FRP composites, including exposure to water, alkaline solutions, saline solutions, elevated temperature, fatigue, creep rupture, and shrinkage. The study examines the implications of these conditions on the physical and mechanical properties of FRP composites and discusses provisions for the serviceability design of FRP-RSC elements. The study concludes that improvements in material properties and more laboratory results contribute to a better understanding of long-term exposure factors, allowing for more confident selection of appropriate factors. The study highlights the key environmental and mechanical conditions that affect the durability and mechanical properties of FRP composites, including exposure to water, alkaline solutions, saline solutions, elevated temperature, fatigue, creep rupture, and shrinkage.

The findings suggest that improvements in material properties and more laboratory results contribute to a better understanding of long-term exposure factors, allowing for more confident selection of appropriate factors. Further research is needed to address cost-related limitations and bendability issues in FRP composites.

## 3.2. Properties of GFRP

GFRP rebars are a promising alternative to traditional steel reinforcement in concrete applications due to their unique characteristics, such as resistance to fatigue and high mechanical performance. These rebars possess a specific gravity roughly one-fourth that of steel, making them highly manoeuvrable during transportation and handling. They also have exceptional electrical and magnetic insulating properties, coupled with a coefficient of thermal expansion comparable to steel. The versatility of GFRP rebars is particularly evident in scenarios necessitating resistance against corrosion, low conductivity, and an impressive strength-to-weight ratio.

The utilization of GFRP rebars often yields cost savings compared to conventional steel-reinforced concrete, while experimental findings affirm their viability in concrete structures. Strategic consideration of reinforcement ratios and height-to-span ratios ensures optimal design. Real-world applications further bolster the credibility of GFRP rebars, as they have been effectively employed in diverse contexts such as sea walls, chemical plants, channel slabs, and concrete tanks without reported issues.

Carbon fibers predominantly dominate in strengthening existing concrete structures, while glass FRP bars are anticipated to thrive in new construction and reconstruction endeavours. Ease of installation stands as a pivotal driver propelling the uptake of FRP technology within the realm of concrete structures. In addition to tests conducted on glass and carbon FRP specimens exposed to various environmental conditions showed outstanding resistance to most factors, except for a decrease in tensile strength due to moisture exposure and a drop in bond strength caused by freeze-thaw cycles.

In addition to, the use of FRP composites as external reinforcement in rehabilitation projects has shown efficiency in improving flexural and shear strength, as well as axial load and ductility

performance. They are particularly attractive for their fast execution and low labour costs. The initial cost of FRP materials and products used in strengthening schemes is perceived as a disadvantage, but a comprehensive evaluation should consider the complete strengthening procedure and life-cycle assessment. FRP reinforcement for concrete structures requires attention to factors such as long-term degradation of mechanical properties, proper selection of FRP material under severe environmental conditions, and bond properties as the governing criteria for deformational analysis.

Finally, FRP composites have several advantages in the structural field, such as high strength, lightweight, and resilience to natural calamities. Their numerous physical qualities, such as density, rigidity, strength-to-weight ratio, and stiffness, make them useful for concrete structure rehabilitation, repair, strengthening, and retrofitting.

## 3.3. Characterization of Mechanical Properties

Tensile strength stands as a fundamental parameter in structural design, determining the maximum axial load a material can withstand without undergoing failure. In the case of GFRP rebars, this property is of paramount importance due to its direct influence on the structural integrity of reinforced elements. The tensile strength of GFRP rebars serves as a basis for evaluating their load-bearing capacity and establishing design parameters to ensure structural safety. As the campaign focuses on GFRP rebars' application in BEC reinforcement, accurate characterization of their tensile strength is pivotal in ensuring their effective use within the specified design context.

### *3.3.1. Codes and Recommendations*

The first step in the experimental campaign involves aligning the testing procedures with established codes and recommendations for GFRP material characterization. Standards and Guidelines such as **CNR-DT 203/2006** [17] The Guide for the Design and Construction of Concrete Structures Reinforced with Fiber-Reinforced Polymer Bars, and the **ISO 10406-1:2008** [18] the International Standard of Fiber-Reinforced Polymer (FRP) Reinforcement of Concrete, outline the test methodologies for determining the tensile properties of GFRP.

These codes provide essential guidelines for specimen preparation, loading rates, and data acquisition, ensuring consistency and accuracy across experimental setups.

**CNR-DT 203/2006 APPENDIX B (TEST METHODS FOR CHARACTERISATING FRP BARS)**[17]

To determine the mechanical properties of a composite bar. The test conditions are with standard environmental conditions (at 23±3 ˚C and 50±10% relative humidity). This test also necessitates the use of at least five FRP specimen bars that have been conditioned in accordance with ASTM 618 procedure A. Prior to testing, the bars must be stored in the test environment for at least 24 hours. The length of the specimens to be tested, $l_p$, shall be in compliance with the following requirements:

$$l_p \geq 100 + 2 \cdot l_a \qquad [length\ in\ mm],$$

$$l_p \geq 40 \cdot d_b + 2 \cdot l_a\ , \qquad (3.1)$$

Considering that $l_a$ and $d_b$ are the length of the anchorage and the bar diameter respectively. The geometry of anchorage systems and, in particular, their length, $l_a$, shall ensure that specimen rupture occurs outside the anchorage zone, whose length equal to, $l_p - 2l_a$.

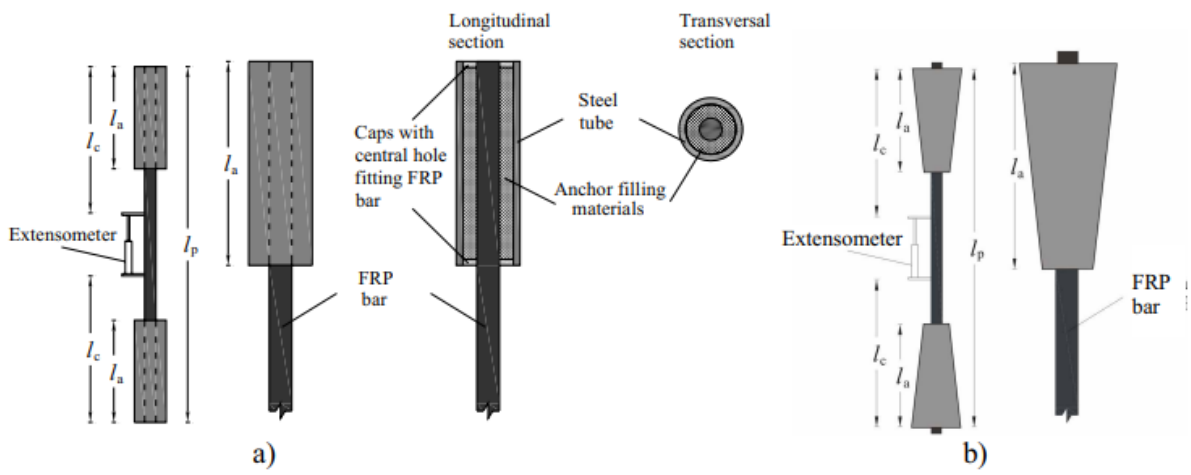


*Figure 3.1: Examples of anchorage devices: a) by using sleet tubes; b) by making cone ends of bar [17].*

Tensile tests in load control, strain control, or displacement control are used to determine the mechanical properties of bars. The test machine's minimum resolution must be 100 N for load, 0.01 for strain, and 0.001 mm for displacement. The rate of load, strain, or displacement must be consistent throughout the test, and the specimen must fail within 1 to 10 minutes. During

the test, the bar strain in the mid-span cross section must be measured using strain gauges or extensometers.

The extensometer's accuracy must be greater than 0.02‰ of the gauge length and not less than 8 times the specimen diameter ($8d_b$). In reference to **Figure 3.1**, therefore the following inequality shall be satisfied: $l_c \geq l_a + 8d_b$.

At the end of the test, the load-strain curve may be obtained from which the tensile strength, $f_{fu,p}$, may be calculated through the following expression:

$$f_{fu,p} = F_{fu,p}/A_b, \tag{3.2}$$

Where $F_{fu,p}$ and $A_b$ represent the recorded ultimate load and the cross-sectional area of the bar, respectively.

The tensile Young's modulus of elasticity, $E_{f,p}$, shall be taken either as a linear regression of the data points from 20 to 50% of the tensile strength of the bar, or alternatively by using the simplified formula:

$$E_{f,p} = \frac{F_1 - F_2}{(\varepsilon_1 - \varepsilon_2) \cdot A_b}, \tag{3.3}$$

Where $F_1$ *and* $\varepsilon_1$ are the load and corresponding strain, respectively, at approximately 50% of the ultimate tensile capacity, while $F_2$ and $\varepsilon_2$, are the load and corresponding strain, respectively, at approximately 20% of the ultimate tensile capacity.

The ultimate strain of the specimen bars, $\varepsilon_{fu,p}$, shall be calculated with the following expression:

$$\varepsilon_{fu,p} = \frac{F_{fu,p}}{E_{f,p} \cdot A_b}, \tag{3.4}$$

Once the mechanical properties of the specimens have been determined, the characteristic values of these properties of the FRP bar may be determined according to Material Properties section in the **CNR-DT 203/2006 [17].**

**ISO 10406-1:2008 Test Method for Tensile Properties** [18] The length of test pieces shall be taken to be the sum of the length of the test section and the anchoring section (see **Figure 3.2**).

For bars, the length of the test section shall be not less than 300 mm, and not less than 40 times the nominal diameter.

The test pieces to be stored carefully and protected against deformation, heating and exposure to ultraviolet light, which can cause changes to the material properties of the test pieces.

The total number of test pieces shall be at least five.

The testing machine should conform to the requirements for the tension-testing machine in accordance with ISO 7500-1.

The anchorage shall be suited to the geometry of the test pieces and shall have the capacity to transmit only the tensile force along the longitudinal axis of the test pieces.

The extensometers and strain gauges used to measure the elongation of the test piece under loading shall be capable of recording variations in the gauge length or elongation during testing with an accuracy of at least $10^{-5}$. The gauge length of the extensometer shall be not less than 100 mm and not less than 8 times the nominal diameter of the FRP bar.

Mount the test piece on the testing machine such that only the axial load in transmitted (see **Figure 3.3**). Mount the extensometer along the axis of the central portion of the test piece.

Carry out the loading in accordance with the following:

1- Apply the load at a constant rate without impact to the test piece. The rate of loading shall be 0.5% to 1.5% strain per minute. The test time shall not exceed 5 min.
2- Measure the strain at not fewer than 10 equally spaced loading increments until approximately two thirds of the maximum tensile force.
3- Record the maximum tensile force with a precision of three significant digits.

The test temperature shall be within the range of 5 ˚C to 35 ˚C.

All results, except for the cases where the location of the failure position is within anchorage, shall be used as a rule. If the failure location is often found to be within anchorage, however, the results of the failure within anchorage may be included. In cases when a result (in terms of the maximum tensile force) deviates by 10% or more from the average value, that result shall be ignored and only the four remaining results shall be used. In such cases, if one result deviates by 10% or more from the average value calculated using the four results, all results shall be rejected and new test shall be performed. Rejected test results shall not be used for the calculation of tensile rigidity, Young's modulus or ultimate strain.

The average, $\bar{x}$, deviation, $\Delta x_i$, and standard deviation, σ, are defined as given in **Equations (3.5) to (3.7)**, respectively:

$$\bar{x} = \frac{1}{N}\sum_{i=1}^{N} x_i \tag{3.5}$$

$$\Delta x_i = x_i - \bar{x} \tag{3.6}$$

$$\sigma = \sqrt{\frac{1}{N}\sum_{i=1}^{N}(x_i - \bar{x})^2} \tag{3.7}$$

where,

$N$ is the number of test pieces;

$x_i$ are the sampling data.

The cross-sectional area shall be the nominal cross-sectional area. If the standard cross-sectional area is reported by the manufacturer of the FRP, the standard cross-sectional area may be used as the cross-sectional area. It is necessary to include the nominal cross-sectional area, effective fiber area, polymer area and fiber strength in the value of the standard cross-sectional area. The tensile strength, $f_u$, expressed in newtons per square millimeter, to a precision of three significant digits using **Equation (3.8)**:

$$f_u = F_u / A \tag{3.8}$$

where,

$F_u$ is the maximum tensile force, expressed in newtons;

$A$ is the cross-sectional area, expressed in square millimetres.

The tensile rigidity, $E_A$, expressed in newtons and Young's modulus, $E$, expressed in newtons square millimeter, both to a precision of three significant digits, using **Equation (3.9)** and **(3.10)**, respectively. It shall be calculated from the difference between the load (stress)-strain curve obtained from the load level at 20% and 50% of the tensile capacity. For materials where a guaranteed tensile capacity is given, the values at 20% and 50% of the guaranteed tensile capacity may be used.

$$E_A = \frac{\Delta F}{\Delta \varepsilon} \tag{3.9}$$

$$E = \frac{\Delta F}{\Delta \varepsilon \times A} \tag{3.10}$$

where,

$\Delta F$ is the difference between loads at 20% and 50% of the maximum tensile force, expressed in newtons;

$\Delta \varepsilon$ is the strain difference for $\Delta F$.

The ultimate strain shall be the strain corresponding to the ultimate tensile capacity when strain-gauge measurements of the test piece are available up to failure. In the event that the measurements from an extensometer or strain gauge are not available up to failure, the ultimate strain, $\varepsilon_u$, shall be calculated to a precision of three significant digits using **Equation (3.11)**:

$$\varepsilon_u = \frac{F_u}{E \times A} \qquad (3.11)$$

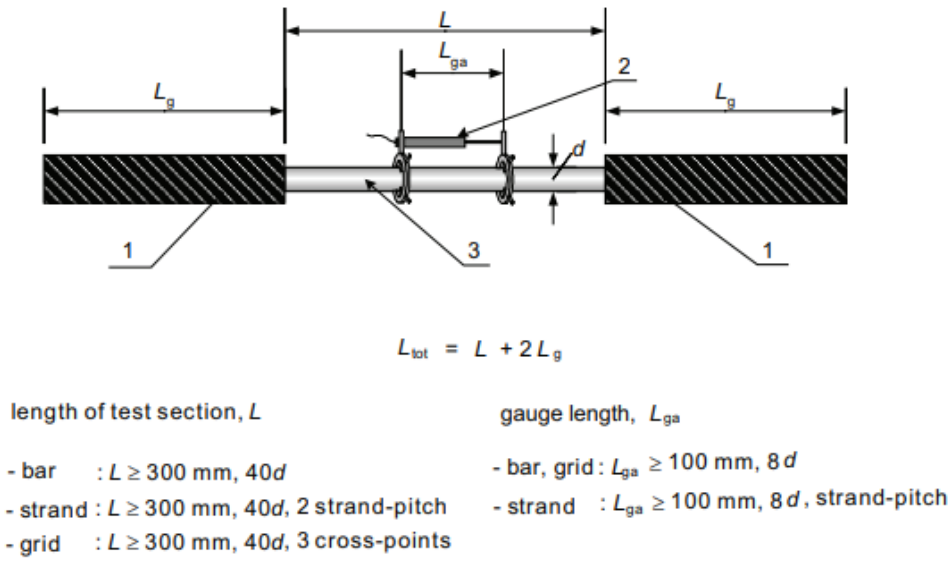


**Key**

1 anchoring section
2 extensometer
3 test section

***Figure 3.2:*** *Test piece for tensile test [18]*

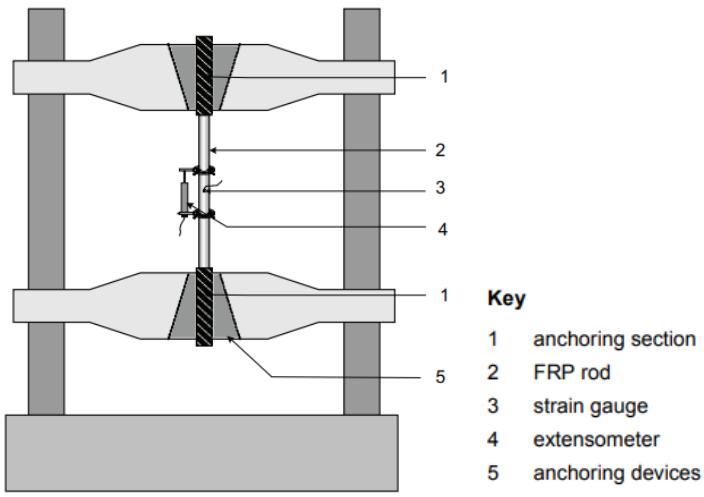


***Figure 3.3:*** *Outline of tensile test [18]*

### *3.3.2. Test Specimens & Setup Preparations*

Collaboration with the manufacturer ATP played a significant role in obtaining the GFRP rebars for the experimental campaign. The manufacturer's expertise and adherence to quality standards ensured the reliability of the materials used in testing. ATP's commitment to delivering GFRP bars of specific diameters—10mm, 12mm, and 16mm—ensured consistency in the specimens subjected to testing.

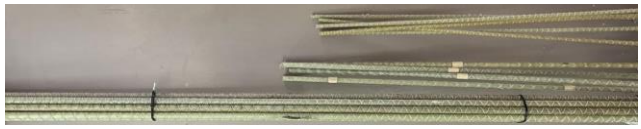

***Figure 3.4:*** *RWB-A-Rebar Φ 16,12,10 mm GFRP Bars (ATP)*

1- **Specimen Length:**

Each GFRP bar was meticulously cut precisely to the desired length in accordance with testing standards and specifications to ensure they free from any irregularities. This step is crucial in guaranteeing uniform loading during the tensile testing process.

Following **Equation (3.1):**

***Table 3.1*** *Φ10,12,16 mm Specimens Length*

| Φ [mm] | Anchoring Length $(l_a)$ $[mm]$ | Bar Length $(l_p)$ $[mm]$ |
|---|---|---|
| 10 | 410 | 1220 |
| 12 | 410 | 1300 |
| 16 | 300 | 1240 |

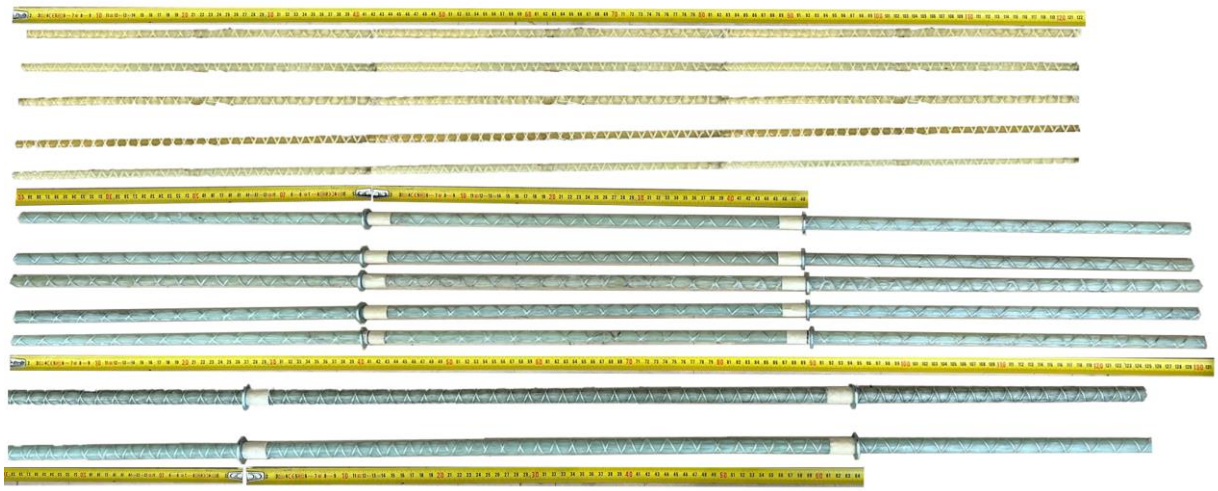

***Figure 3.5:*** *Bars Φ10,12,16 mm Dimensions after Cut*

**2- Anchoring System:**

The steel tubes, integral components of the anchoring system, were meticulously cut to the required dimensions. Following the cutting process, the steel tubes underwent a thorough cleaning regimen. This step involved the removal of any contaminants that could hinder the tubes' interaction with the epoxy resin. A clean surface is paramount to ensuring proper adhesion and load transfer within the anchoring system.

***Figure 3.6:*** *Bars Φ10,12 400 mm Length Steel Tube Anchors, Bars Φ16 300 mm Length Steel Tube Anchors*

**3- Compilation of the Rebar and the Steel Anchors:**

The assembly process involves the meticulous compilation of both the GFRP rebars and the steel anchors. Flat washers with the same inner diameter as the external diameter of the bars have been bonded to the anchors to help with the strategically positioning of the steel anchors in their concentric designated locations as shown in the previous figure (**Figure 3.6**). A crucial step follows to ensure a seamless epoxy resin pouring process and prevent any undesired dripping, a specialized sealing technique is employed.

To prepare for the subsequent epoxy resin pouring process, a meticulous sealing step is implemented. Specifically, wax is utilized to seal the openings and gaps between the GFRP rebars and the steel anchors. This sealing action serves two critical purposes: first, it prevents any potential dripping during the epoxy resin application, ensuring a controlled and even distribution; second, it fixating the steel anchor in the designed position, until the full curing of the epoxy resin.

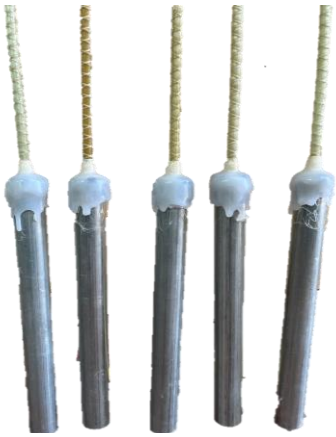

***Figure 3.7:*** *Installing and Waxing the First Side of the Steel Anchors for Pouring Epoxy Resin Process*

**4- Epoxy Resin Application:**

After the full curing of the wax, the rebars should be hanged for resin pouring process and to give the freedom to the rebar until the full curing of the epoxy to ensure the axial alignment of the rebar without the effect of any external actions.

Repeat the whole steps once again to the other side after the full curing of the epoxy resin in the first side.

- **Mild Steel Tubes Anchors**

  The resin used with this type of anchor is Epoxy EPOJET **09 CPR-IT1/0095.** The wax sealing technique is mandatory for this type of resin, because it is in liquid state until curing.

- **Self-drilling Hollow Bars with Continuous Thread Steel Tubes Anchors**

  The resin used with this type of anchors is Epoxy MAPEFIX EP 100 **N.CPR-IT1/0921.** Which is hardener than **09 CPR-IT1/0095** but more expensive, and it is in paste state where we can exclude the wax technique saving time and materials.


(a) (b)

***Figure 3.8:*** *a) EPOJET **09 CPR-IT1/0095** Epoxy Resin & Hardner; b) MAPEFIX EP 100 **N.CPR-IT1/0921** Epoxy Resin & Hardner*

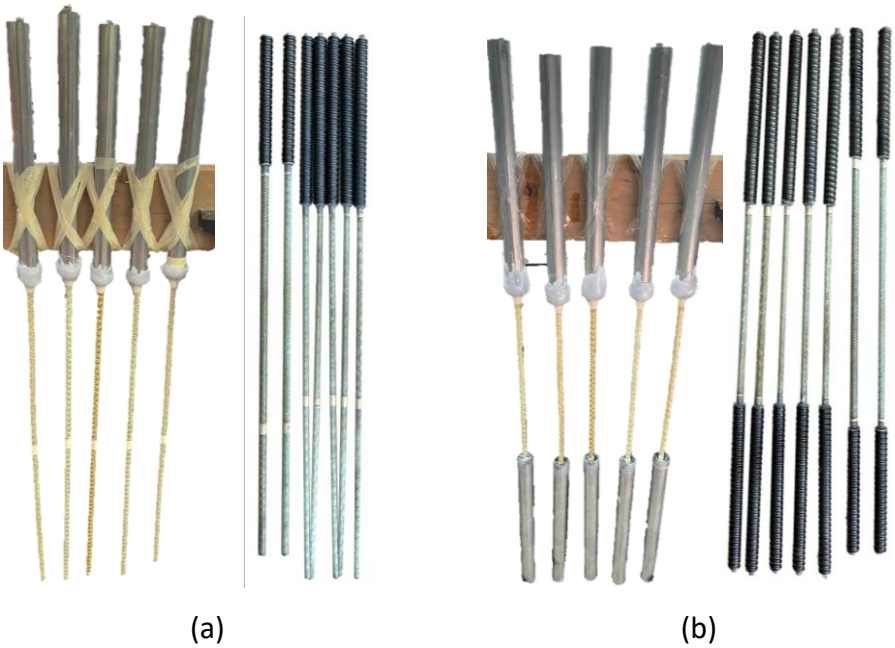


***Figure 3.9:*** *a) The rebars Hanged for resin pouring in the first side; b) The rebars Hanged for resin pouring in the other side.*

**5- Strain Gauge Installation:**

During installation, Strain gauge is carefully bonded to the surface of the specimen at predetermined position within the mid-span cross section. This position is strategically selected to capture strains along tension zone, allowing for a comprehensive understanding of the specimen behavior.

***Figure 3.10:*** *Strain Gauge Bonded to Rebars*

(a) (b) (c) (d)

***Figure 3.11:*** *a) 2Φ16 mm Specimens Ready for Test [Spiral Anchors]; b) 5Φ12 mm Specimens Ready for Test [Spiral Anchors]; c) 5Φ10 mm Specimens Ready for Test [Mild Steel Anchors]; d) 5Φ12 mm Specimens Ready for Test [Mild Steel Anchors]*

### *3.3.3. Test & Results*

After install the extensometer at the middle of the specimen, a tensile test in displacement control was performed.

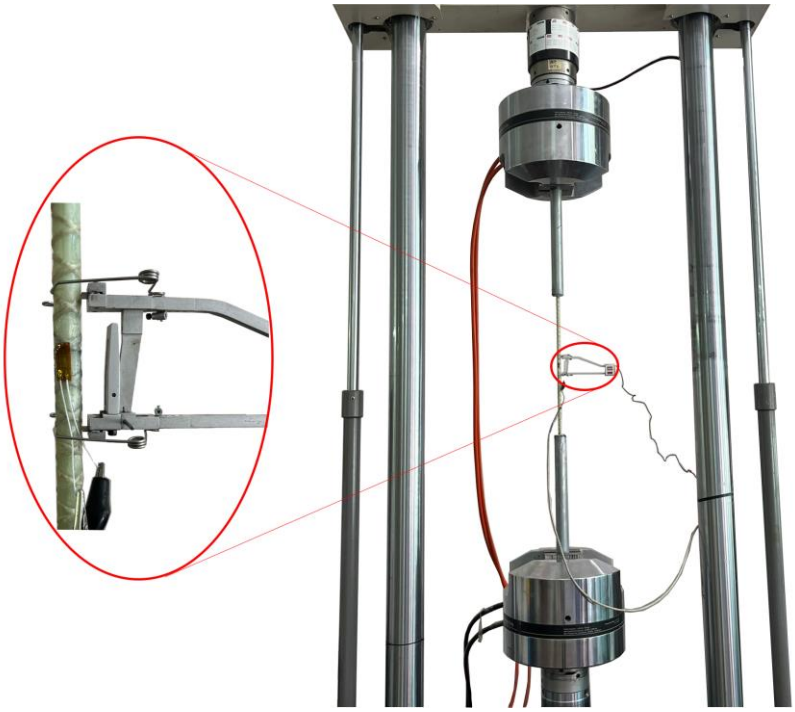

***Figure 3.12:*** *The installation of the specimen in the machine*

**A) Test with Mild Steel Anchors**

**5 Φ 10 mm**

A tensile test in displacement control with a rate of **2 mm/min** was performed. Three out of the five specimen failed due to debonding occurred during the test.

***Figure 3.13:*** *The non-acceptable Debonding Failure of 3 Φ 10 mm Specimens*

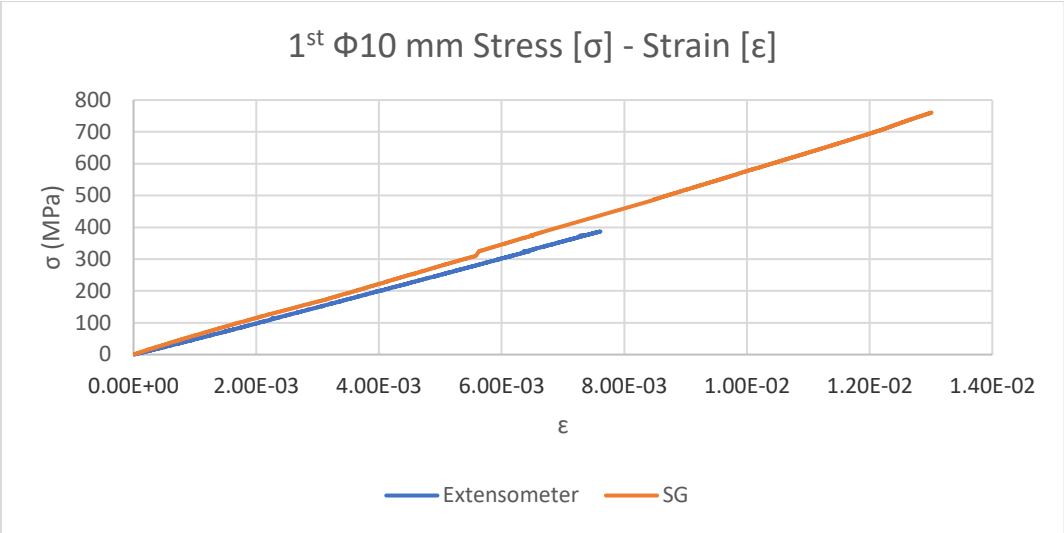


***Figure 3.14:*** *Φ10 mm 1st Specimen [Stress-Strain] Curve*

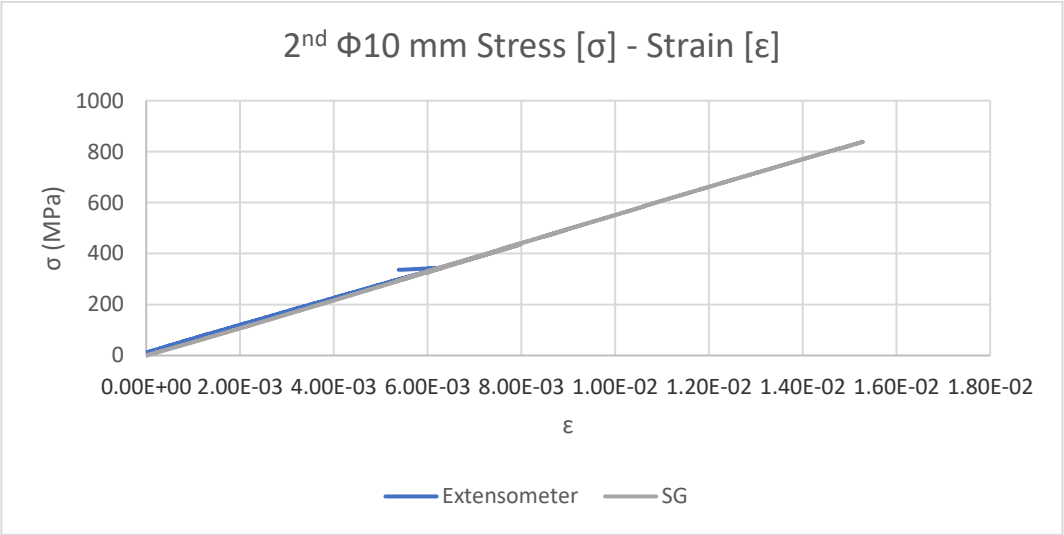


***Figure 3.15:*** *Φ10 mm 2nd Specimen [Stress-Strain] Curve*

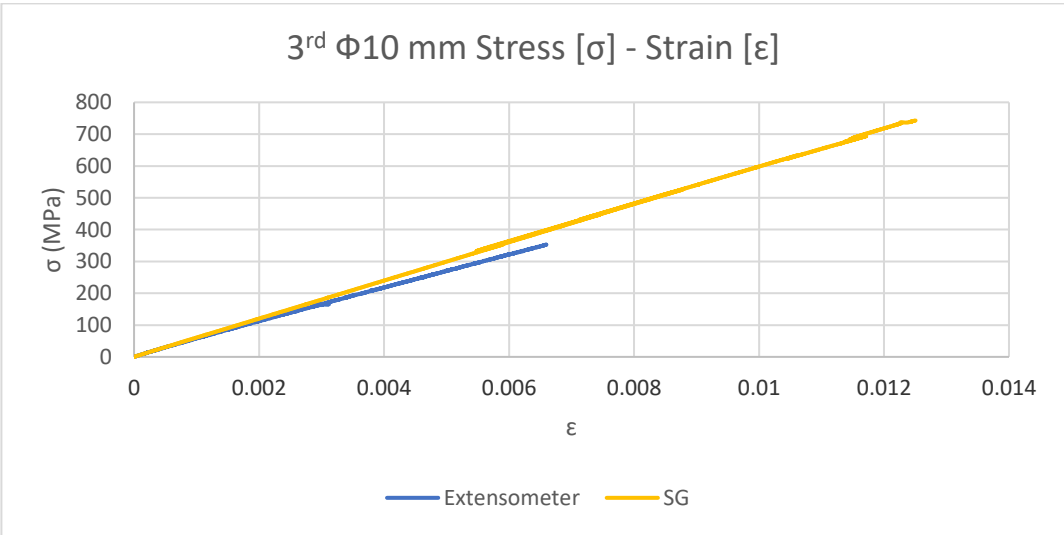


***Figure 3.16:*** *Φ10 mm 3rd Specimen [Stress-Strain] Curve*

The remaining two specimens' failure was acceptable although they aren't enough to define the tensile strength of Φ 10 mm GFRP rebars.

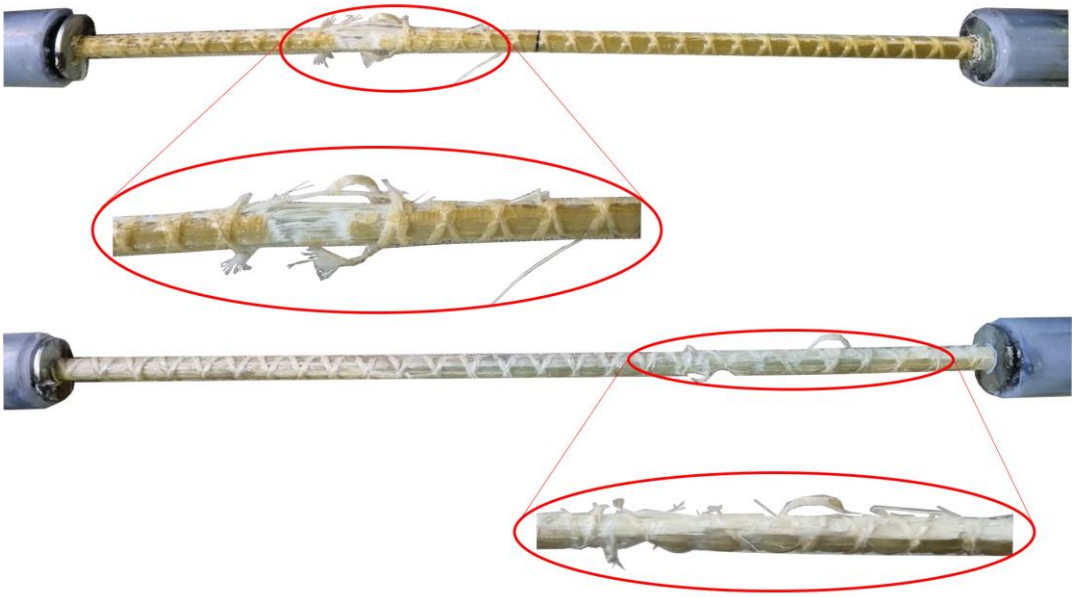

***Figure 3.17:*** *The Acceptable Fiber Rupture Failure of 2 Φ 10 mm Specimens*

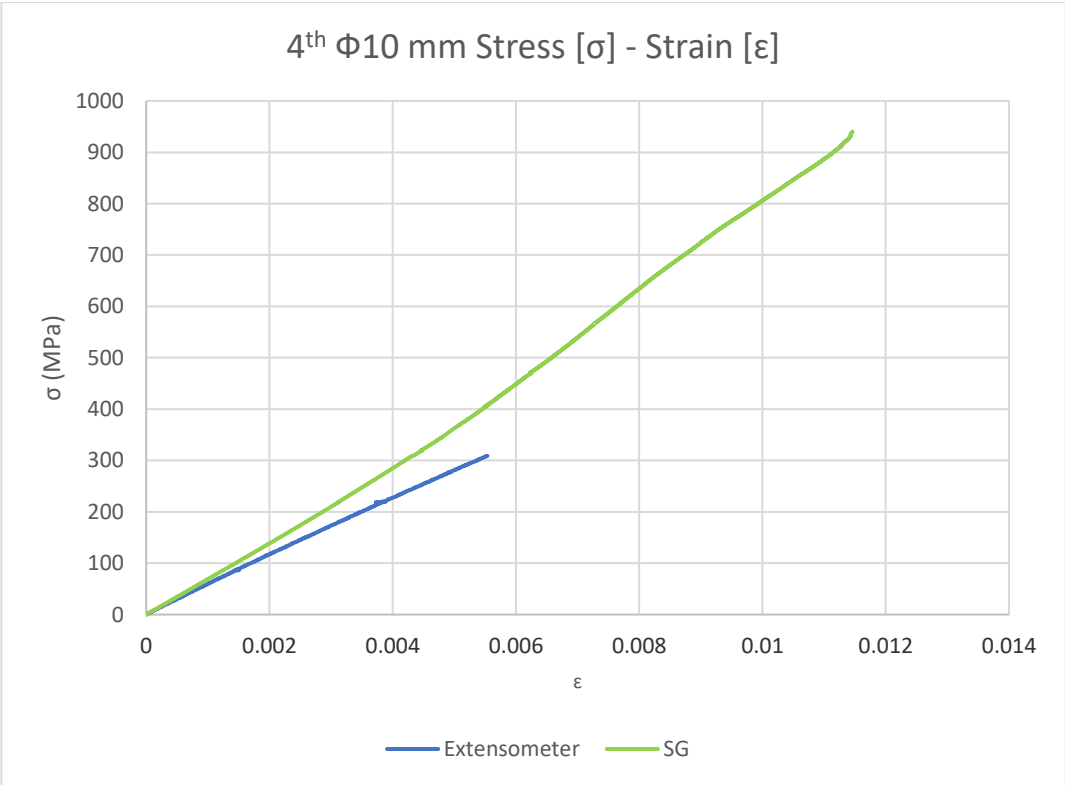


***Figure 3.18:*** *Φ10 mm 4th Specimen [Stress-Strain] Curve*

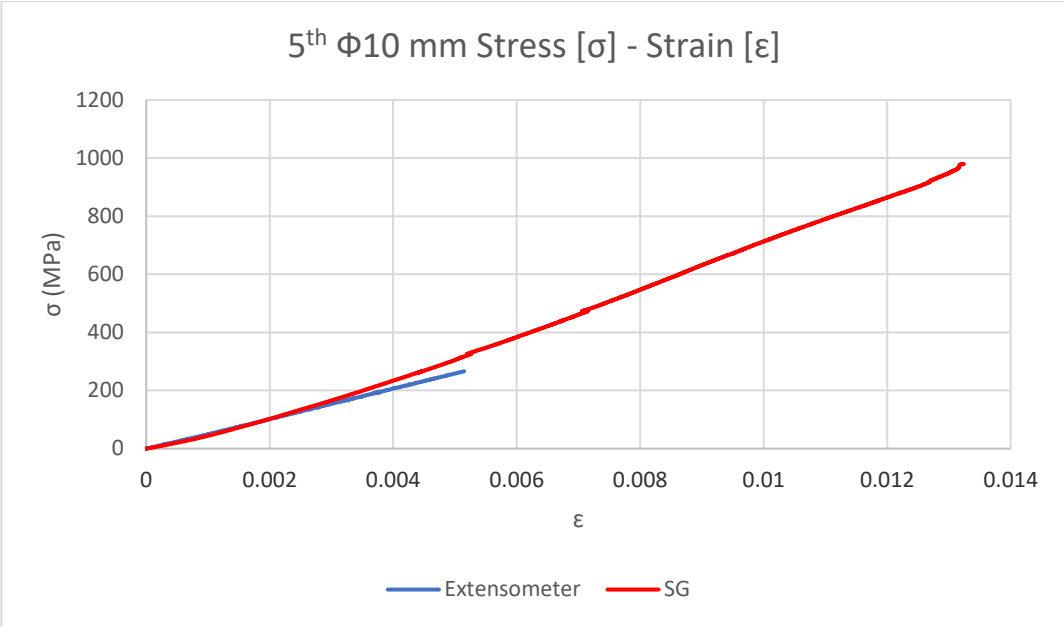


***Figure 3.19:*** *Φ10 mm 5th Specimen [Stress-Strain] Curve*

***Table 3.2*** *5 Φ 10 mm Tensile Test Results*

| Φ 10 [mm] | Max. Load $F_{ult.,i}$ [kN] | Max. Stress $\sigma_{ult.,i}$ [MPa] | Max. Strain $\varepsilon_{ult.,i}$ | Modulus of Elasticity $E_i$ [GPa] | Failure Type |
|---|---|---|---|---|---|
| 1st | 59.72 | 760.38 | 0.0119 | 59.01 | Debonding |
| 2nd | 65.86 | 838.55 | 0.0152 | 55.11 | Debonding |
| 3rd | 58.35 | 742.96 | 0.0124 | 60.08 | Debonding |
| 4th | 73.86 | 940.47 | 0.0118 | 79.44 | Fiber Rupture |
| 5th | 76.92 | 979.38 | 0.0128 | 76.57 | Fiber Rupture |

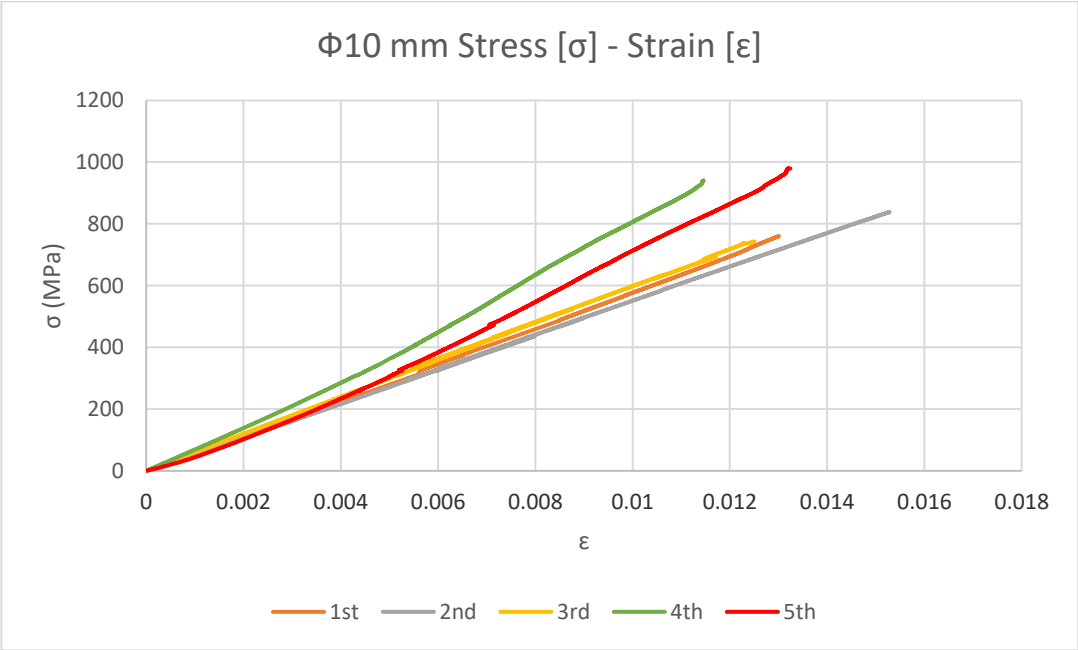


***Figure 3.20:*** *5Φ10 mm Specimens [Stress-Strain] Curve*

**5 Φ 12 mm**

A tensile test in displacement control with a rate of **2 mm/min** was performed.

The whole five specimen failed due to debonding occurred during the test.

***Figure 3.21:*** *The non-acceptable Debonding Failure of 5 Φ 12 mm Specimens*

**B) Test with Spiral Anchors**

**5 Φ 12 mm**

A tensile test in displacement control with a rate of **3 mm/min** was performed.

Four out of five specimens' failure was acceptable, and the results were used to define the tensile strength of Φ 12 mm GFRP Rebars.

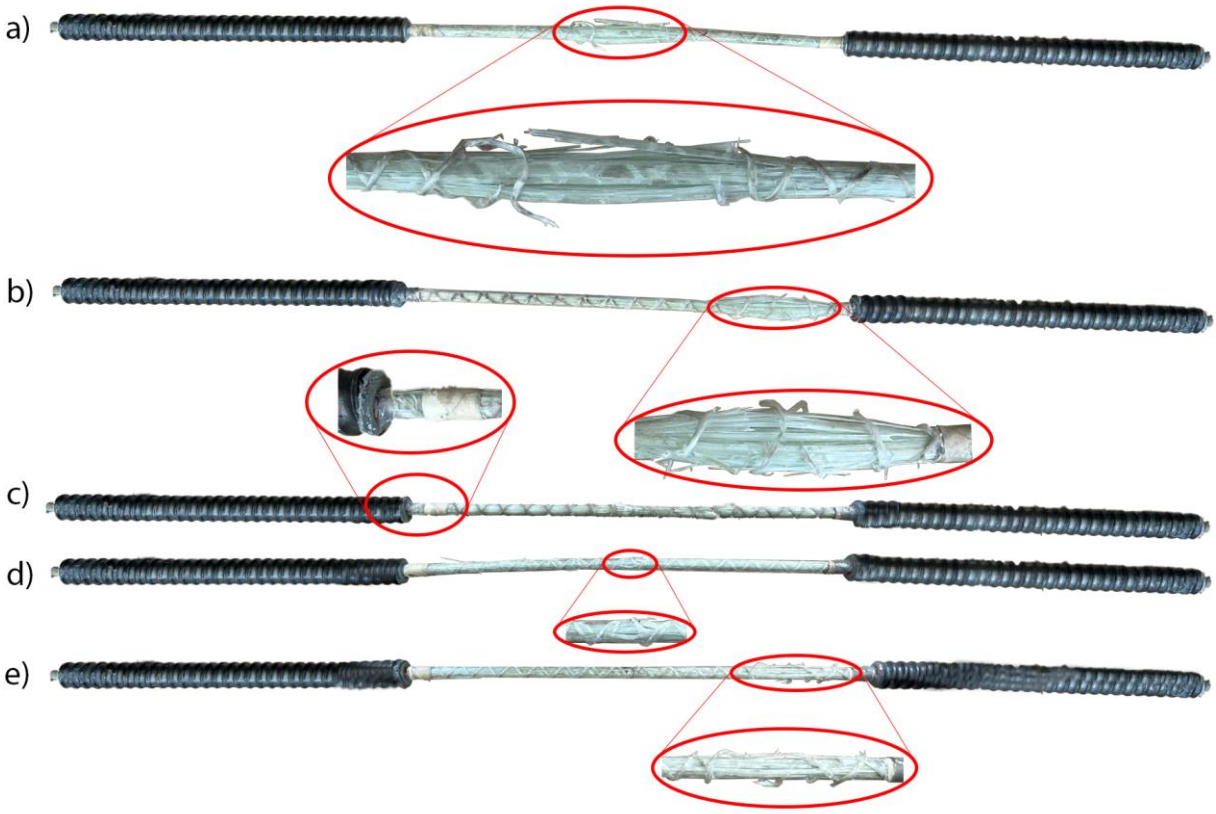


***Figure 3.22:*** *a);b);d);e) 1st, 2nd, 4th, 5th Φ12mm specimens with acceptable Fiber Rupture Failure; c) 3rd Φ12mm specimens with non-acceptable Debonding Failure*

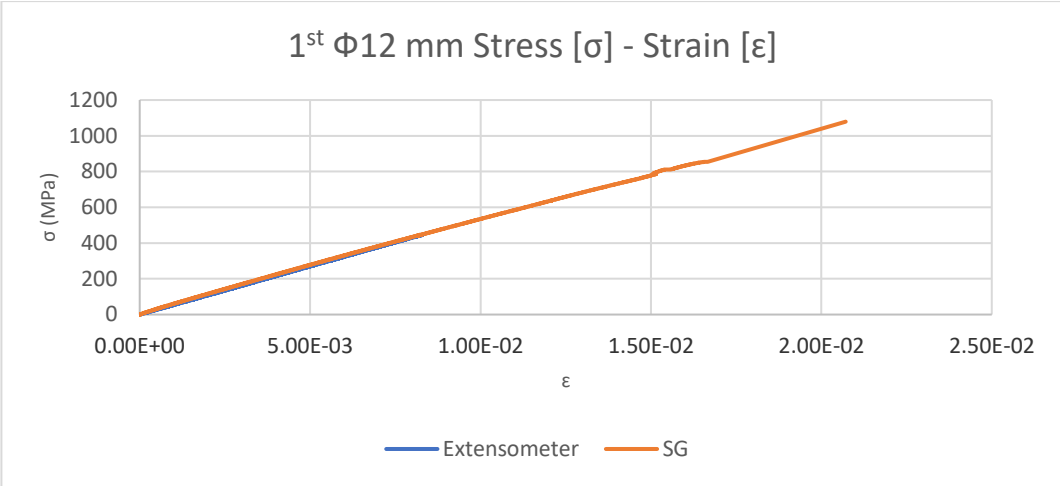


***Figure 3.23:*** *Φ12 mm 1st Specimen [Stress-Strain] Curve*

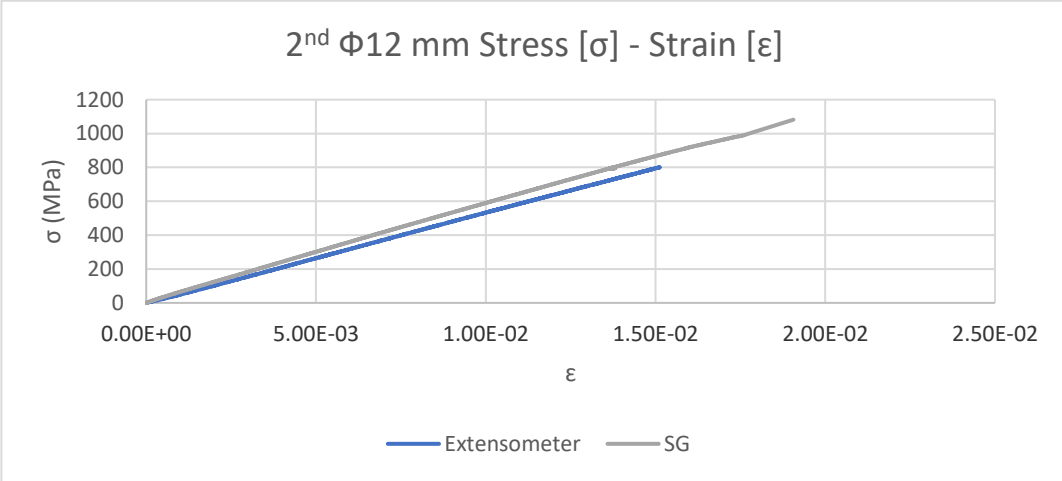


***Figure 3.24:*** *Φ12 mm 2nd Specimen [Stress-Strain] Curve*

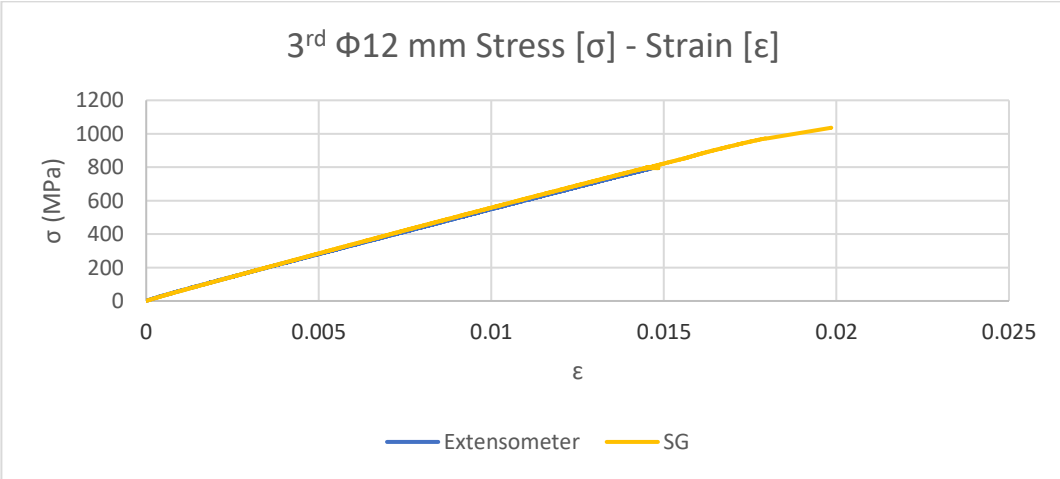


***Figure 3.25:*** *Φ12 mm 3rd Specimen [Stress-Strain] Curve*

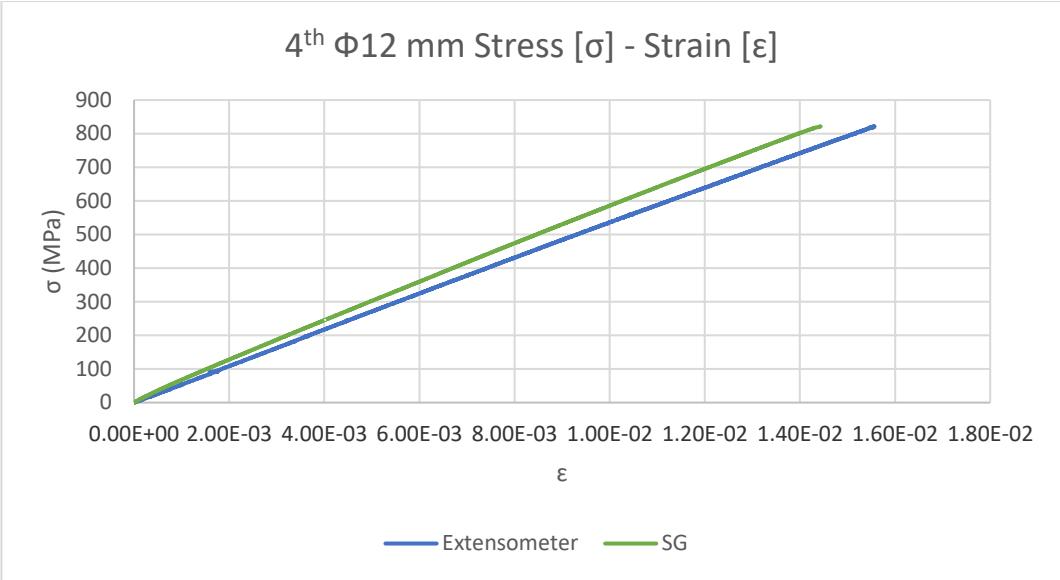


***Figure 3.26:*** *Φ12 mm 4th Specimen [Stress-Strain] Curve*

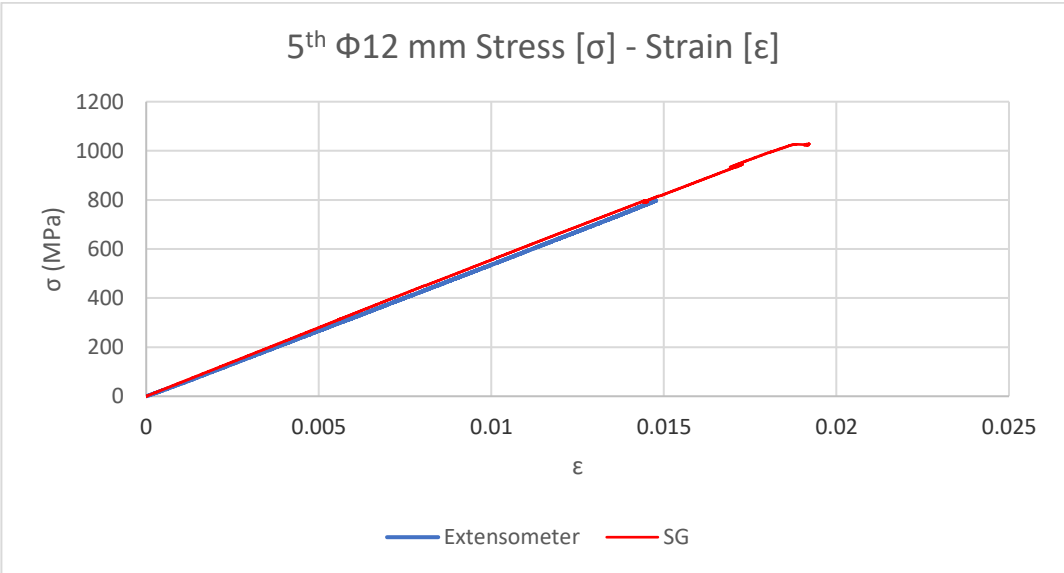


***Figure 3.27:*** *Φ12 mm 5th Specimen [Stress-Strain] Curve*

***Table 3.3*** *5 Φ 12 mm Tensile Test Results*

| Φ 12 [mm] | Max. Load $F_{ult.,i}$ [kN] | Max. Stress $\sigma_{ult.,i}$ [MPa] | Max. Strain $\varepsilon_{ult.,i}$ | Modulus of Elasticity $E_i$ [GPa] | Failure Type |
|---|---|---|---|---|---|
| 1st | 122.03 | 1079 | 0.0209 | 51.74 | Fiber Rupture |
| 2nd | 122.35 | 1081.83 | 0.0186 | 58.17 | Fiber Rupture |
| 3rd | 117.15 | 1035.85 | 0.0188 | 55.06 | Fiber Rupture |
| 4th | 92.94 | 821.73 | 0.0142 | 57.75 | Debonding |
| 5th | 116.3 | 1028.28 | 0.0186 | 55.37 | Fiber Rupture |

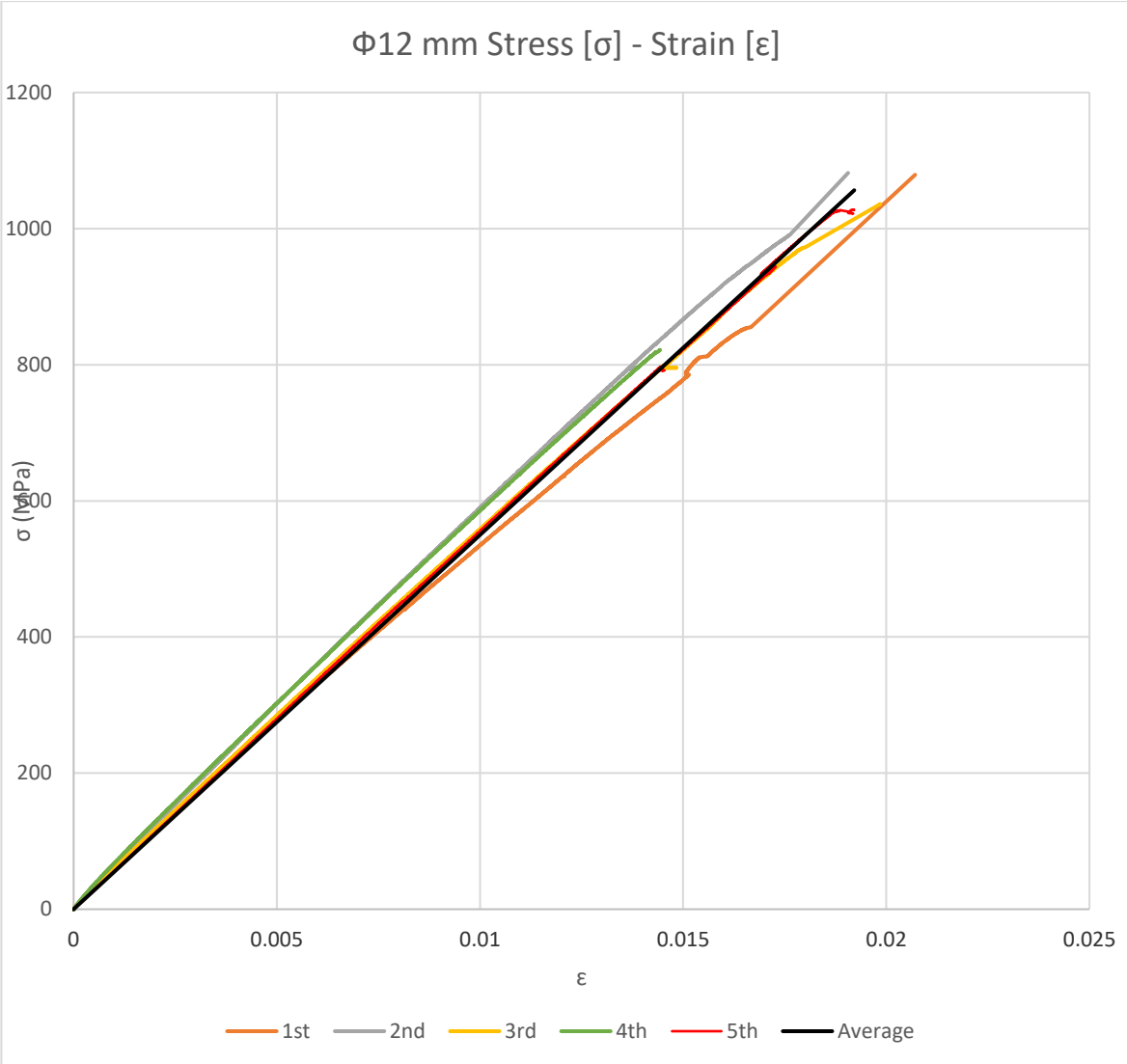


***Figure 3.28:*** *5Φ12 mm Specimens [Stress-Strain] Curve*

***Table 3.4*** *Φ12mm GFRP Rebars Experimental Mean Values of σ, ε, and E*

| Max. Stress $\sigma_{ult}$ [MPa] | | Max. Strain $\varepsilon_{ult}$ | | Modulus of Elasticity **E** [GPa] | |
|---|---|---|---|---|---|
| Mean Value | COV % | Mean Value | COV % | Mean Value | COV % |
| 1056.24 | 2.66 | 0.0192 | 5.74 | 55.085 | 4.78 |

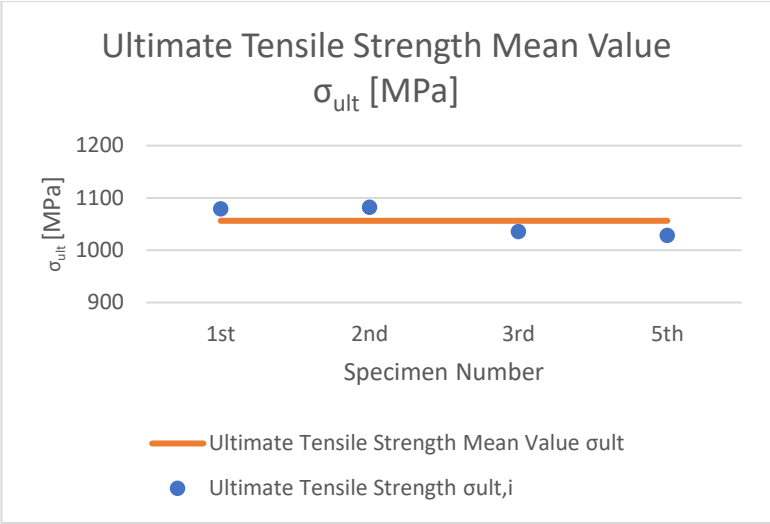


***Figure 3.29:*** *The Ultimate Tensile Strength of Each Specimen and The Mean Value in MPa*

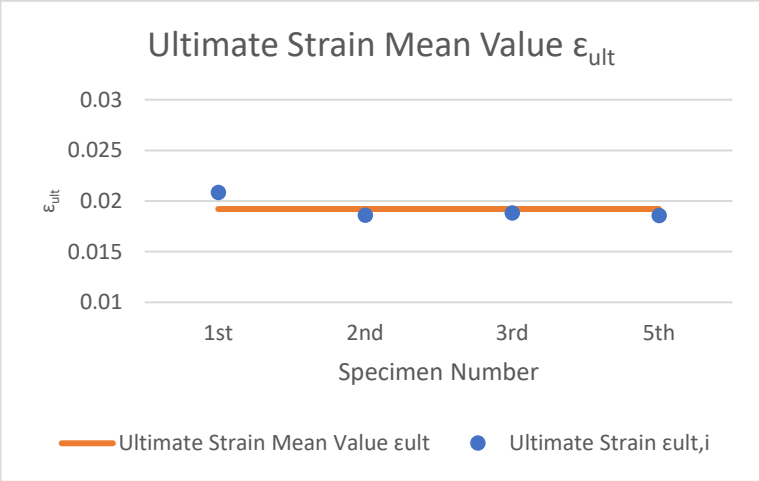


***Figure 3.30:*** *The Ultimate Strain of Each Specimen and The Mean Value*

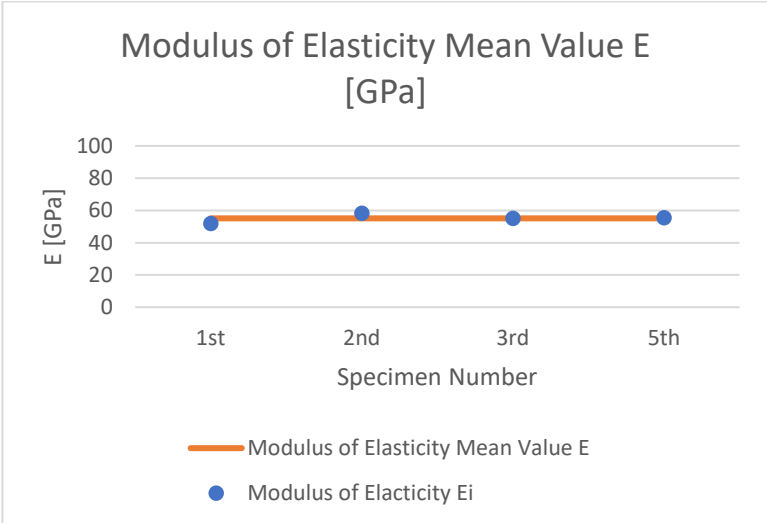


***Figure 3.31:*** *The modulus of Elasticity of Each Specimen and The Mean Value in GPa*

**2 Φ 16 mm**

A tensile test in displacement control with a rate of **5 mm/min** was performed at Φ 16 mm to check the test setup for this particular diameter.

One specimen's failure was acceptable Fiber rupture while the other specimen's failure was non-acceptable debonding failure.

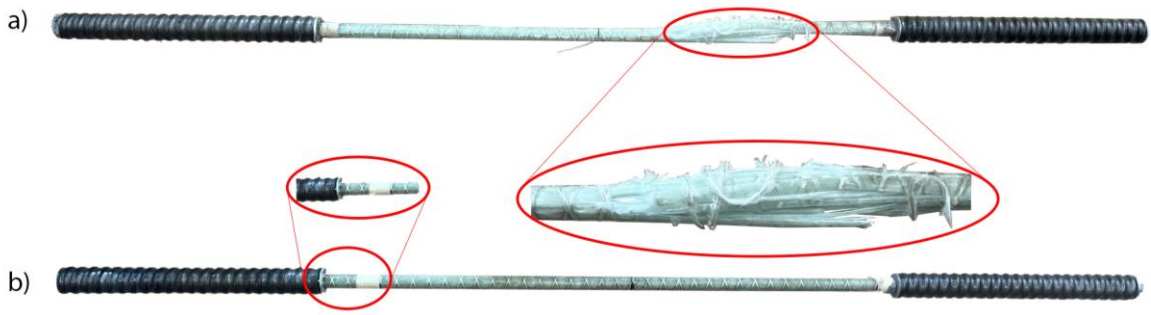


***Figure 3.32:*** *a) Φ16mm specimens with acceptable Fiber Rupture Failure; b) Φ16mm specimens with non-acceptable Debonding Failure*

We noticed that the debonding failure occurred in the second specimen was between the fibers, not between the bar and the anchors as shown in **Figure 3.33** which may be because a not very high quality of the specific tested rebar.

***Figure 3.33:*** *The debonding occurred between the fibers in Φ 16mm 2nd specimen*

***Table 3.5*** *2 Φ 16 mm Tensile Test Results*

| Φ 16 [mm] | Max. Load $F_{ult.,i}$ [kN] | Max. Stress $\sigma_{ult.,i}$ [MPa] | Max. Strain $\varepsilon_{ult.,i}$ | Modulus of Elasticity $E_i$ [GPa] | Failure Type |
|---|---|---|---|---|---|
| 1st | 182.12 | 905.8 | 0.0152 | 59.75 | Fiber Rupture |
| 2nd | 175.5 | 872.6 | 0.0144 | 60.42 | Debonding |

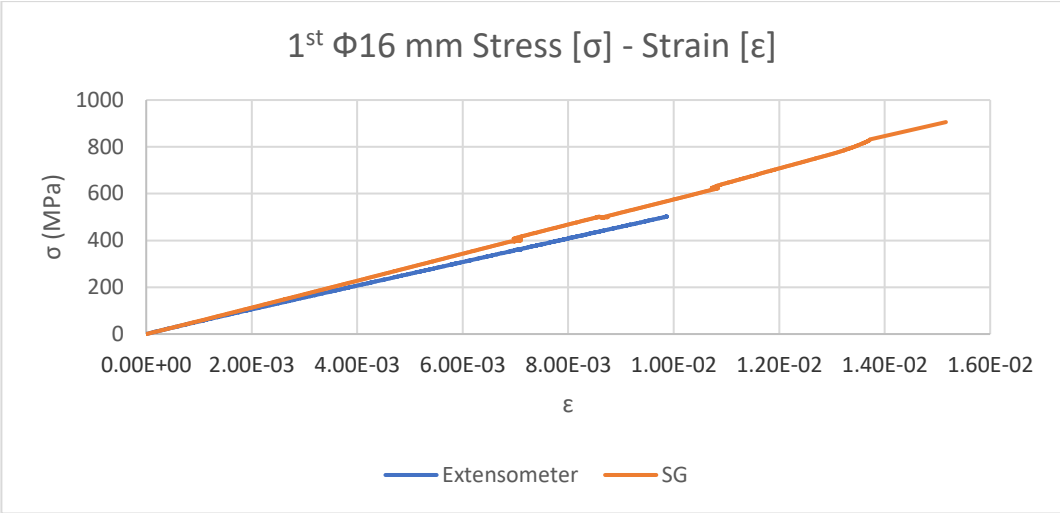


***Figure 3.34:*** *Φ16 mm 1st Specimen [Stress-Strain] Curve*

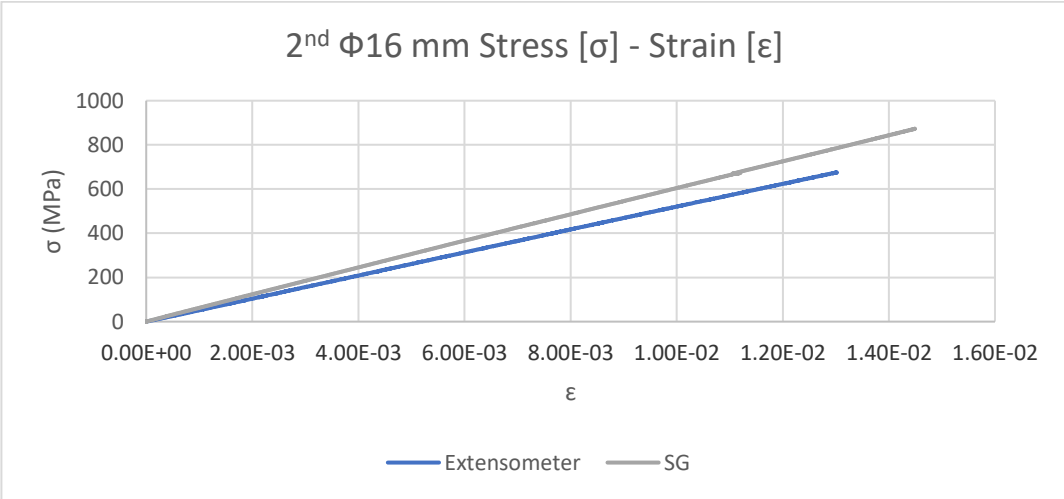


***Figure 3.35:*** *Φ16 mm 2nd Specimen [Stress-Strain] Curve*

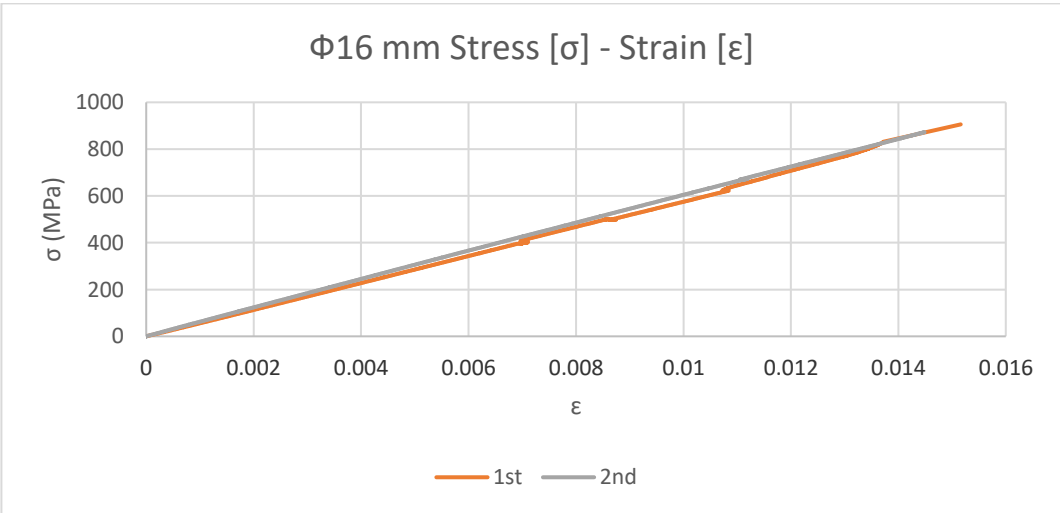


***Figure 3.36:*** *2 Φ16 mm Specimens [Stress-Strain] Curve*

***Table 3.6*** *Summary of all the tests performed (Accepted specimens highlighted)*

| Group | | Ult. Tensile Load | Ult. Tensile Stress | Ult. Tensile Strain | Modulus of Elasticity | Failure Type |
|---|---|---|---|---|---|---|
| | | $F_{ult.,i}$ [kN] | $\sigma_{ult.,i}$ [MPa] | $\varepsilon_{ult.,i}$ | $E_i$ [GPa] | |
| Φ 10 [mm] | 1st | 59.72 | 760.38 | 0.0119 | 59.01 | Debonding |
| | 2nd | 65.86 | 838.55 | 0.0152 | 55.11 | Debonding |
| | 3rd | 58.35 | 742.96 | 0.0124 | 60.08 | Debonding |
| | 4th | 73.86 | 940.47 | 0.0118 | 79.44 | Fiber Rupture |
| | 5th | 76.92 | 979.38 | 0.0128 | 76.57 | Fiber Rupture |
| Φ 12 [mm] | 1st | 122.03 | 1079 | 0.0209 | 51.74 | Fiber Rupture |
| | 2nd | 122.35 | 1081.83 | 0.0186 | 58.17 | Fiber Rupture |
| | 3rd | 117.15 | 1035.85 | 0.0188 | 55.06 | Fiber Rupture |
| | 4th | 92.94 | 821.73 | 0.0142 | 57.75 | Debonding |
| | 5th | 116.3 | 1028.28 | 0.0186 | 55.37 | Fiber Rupture |
| Φ 16 [mm] | 1st | 182.12 | 905.8 | 0.0152 | 59.75 | Fiber Rupture |
| | 2nd | 175.5 | 872.6 | 0.0144 | 60.42 | Debonding |

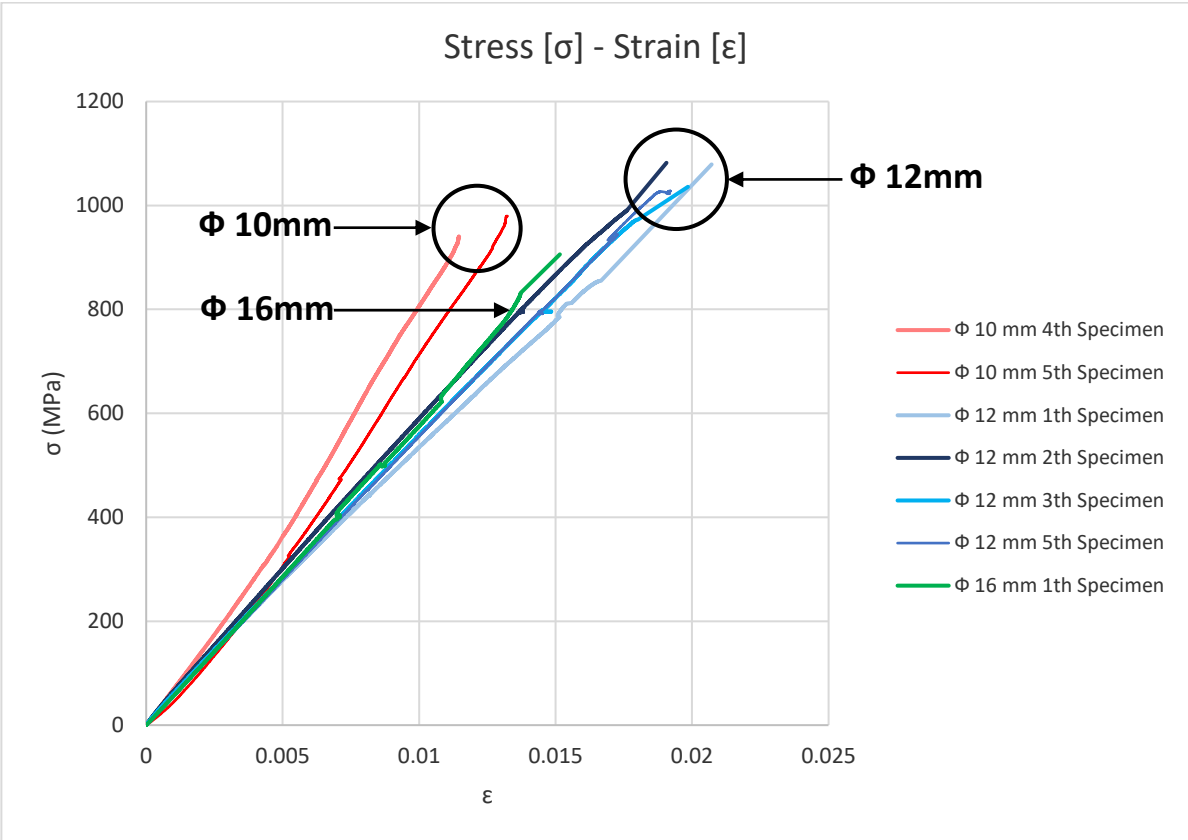


***Figure 3.37:*** *Summary of all the accepted specimens*

THIS PAGE WAS INTENTIONALLY LEFT BLANK

# 4. Design and Verifications of Bridge Edge Curb with GFRP Rebars

## 4.1. Configurations

### *4.1.1. Pre intervention Configuration*

The existing BEC, with steel reinforcement rebars is depicted in **Figure 4.1**, showcasing the longitudinal and transverse steel reinforcement configuration, and the most exposed regions to moisture and corrosion.

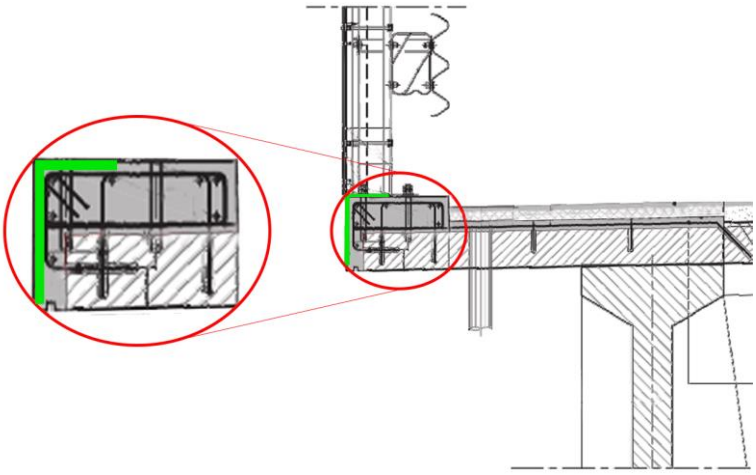

***Figure 4.1:*** *Configuration of BEC with Steel reinforcement rebars*

The anchors used for connecting the BEC with bridge slab are installed each 0.5 m along the edge curb as shown in **Figure 4.2**.

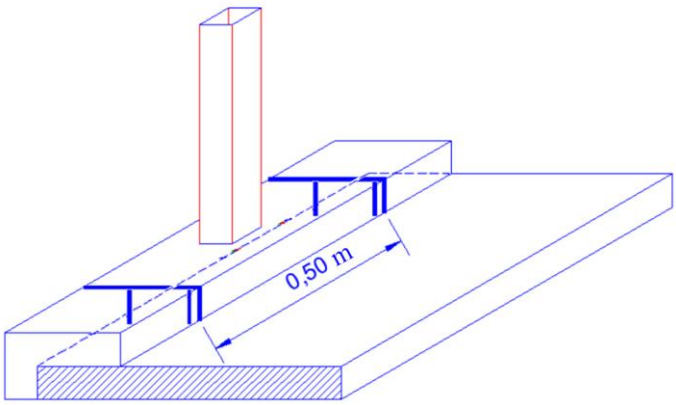


***Figure 4.2:*** *Position of anchors along the bridge edge curb.*

### *4.1.2. Post intervention Configuration*

The proposed configuration of the BEC, or Bridge Edge Curb, after intervention involves the replacement of traditional steel reinforcements with Glass Fiber Reinforced Polymer (GFRP) reinforcements, as depicted in **Figure 4.3**. This innovative change aims to enhance the curb's durability while reducing maintenance needs and increasing resistance to corrosion. The GFRP reinforcement is a sustainable alternative that offers excellent structural performance, ensuring the long-term safety and reliability of the bridge edge curb.

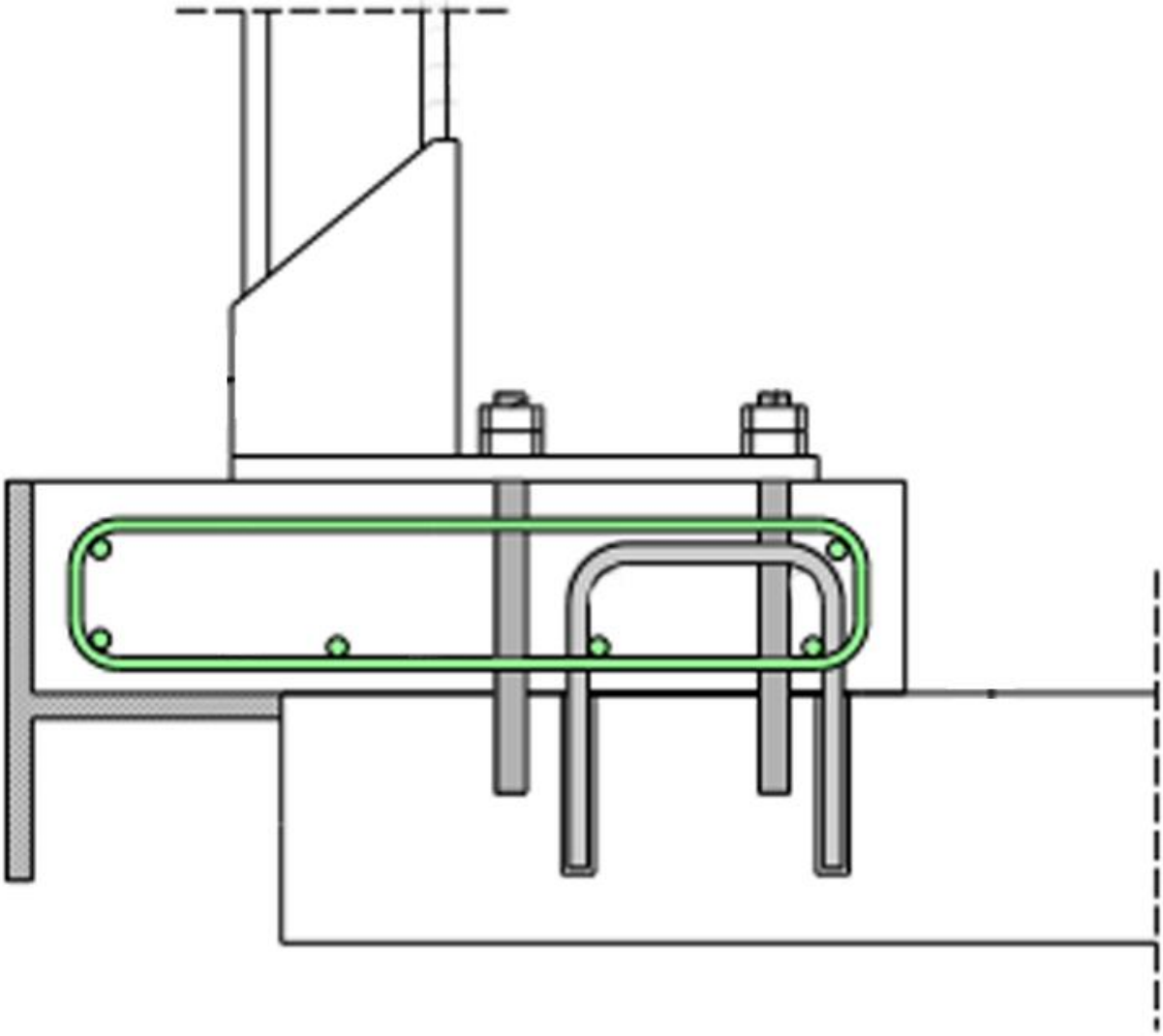

***Figure 4.3:*** *The proposed design configuration for the BEC with GFRP rebars*

## 4.2. Application

This section encompasses the utilization of results derived from the experimental tests to facilitate the design of the Bridge Edge Curb (BEC) with (GFRP) reinforcements. These results serve as fundamental inputs for formulating the design parameters, ensuring that the BEC is structurally robust and resilient. By extrapolating the mechanical properties of GFRP rebars acquired through experimentation, the section encompasses the formulation of a design strategy for the BEC that integrates GFRP reinforcements. This strategy involves optimizing the proposed geometry of the BEC while adhering to the critical impact stability check. The outcome is the determination of the minimum GFRP reinforcements needed, effectively aligning the BEC's design with safety, load-bearing capacity, and durability objectives.

### *4.2.1. Design Material Properties*

**Concrete**

Concrete **C28/35** was used in this design. According to **CNR-DT 203/2006** [17], and **EN 1992-1-1:2004** [19] the following formulas was used to calculate the design values of the concrete resistance.

$$f_{ctm} = 0.30 {f_{ck}}^{(2/3)} \quad (4.1)$$

$$f_{cm} = f_{ck} + 8\ MPa \quad (4.2)$$

$$E_{cm} = 22(F_{cm}/10)^{0.3}\ , F_{cm}\ in\ [MPa] \quad (4.3)$$

$$f_{cd} = \alpha_{cc} \frac{f_{ck}}{\gamma_c} \quad (4.4)$$

Where

$f_{ck}$ : Characteristic compressive cylinder strength of concrete at 28 days.

$f_{ctm}$: Mean value of axial tensile strength of concrete.

$f_{cm}$ : Mean value of concrete cylinder compressive strength.

$E_{cm}$ : Secant modulus of elasticity of concrete.

$f_{cd}$ : Design value of concrete compressive strength.

$\varepsilon_{cu}$ : Ultimate concrete compressive strain.

$\alpha_{cc}$ : is the coefficient taking account of long-term effects on the compressive strength and of unfavorable effects resulting from the way the load is applied.

The value of $\boldsymbol{\alpha_{cc}}$ for use in a Country should lie between 0.8 and 1.0 and may be found in its National Annex. The recommended value is 1 according to **EN 1992-1-1:2004** [19].

$\gamma_c$ : The partial safety factor for concrete.

***Table 4.1*** *Partial Factors for Materials for Ultimate Limit States According to EN 1992-1-1 [19]*

| Design Situations | $\gamma_c$ For Concrete | $\gamma_s$ For Reinforcing Steel | $\gamma_s$ For Prestressing Steel |
|---|---|---|---|
| Persistent & Transient | 1.5 | 1.15 | 1.15 |
| Accidental | 1.2 | 1.0 | 1.0 |

***Table 4.2*** *Concrete C28/35 Design Material Properties*

| $f_{ck}[MPa]$ | $f_{ctm}[MPa]$ | $f_{cm}[MPa]$ | $E_{cm}[GPa]$ | $f_{cd}[MPa]$ | | $\varepsilon_{cu}$ |
|---|---|---|---|---|---|---|
| 28 | 2.77 | 36 | 32.31 | $\alpha_{cc} = 0.85$ | $\gamma_c = 1.5$ | 0.0035 |
| | | | | 15.87 | | |

**GFRP**

According to the tensile test results, the mean value of the tensile strength $\boldsymbol{f_{ftm}}$ **(Table 3.4)** has been calculated. In order to determine the design tensile strength of FRP reinforcement $\boldsymbol{f_{ftd}}$, it's required to define the characteristic tensile strength value of FRP reinforcement $\boldsymbol{f_{ftk}}$. Based on **prEN 1990** [20] the characteristic value of the resistance (5% fractile) $\boldsymbol{f_{ftk,0}}$ can be calculated by the following:

$$f_k = f_m \cdot exp\left\{-k_n \cdot \sqrt{ln\left(1 + V_{exp}{}^2\right)} - \frac{ln\left(1+V_{exp}{}^2\right)}{2}\right\} \qquad (4.5)$$

Where

$f_k$ : The characteristic value.

$f_m$ : The mean value. $f_m = 1056.24\ MPa$ ($\boldsymbol{Table\ 3.4}$).

$k_n$ : The characteristic fractile factor. $k_n = 2.63$ ($\boldsymbol{Table\ 4.3}$).

$V_{exp}$: The experimental coefficient of variation. $V_{exp} = 0.0266$ ($\boldsymbol{Table\ 3.4}$).

The stress-strain relationship should be taken as illustrated in **(Figure 4.4)**

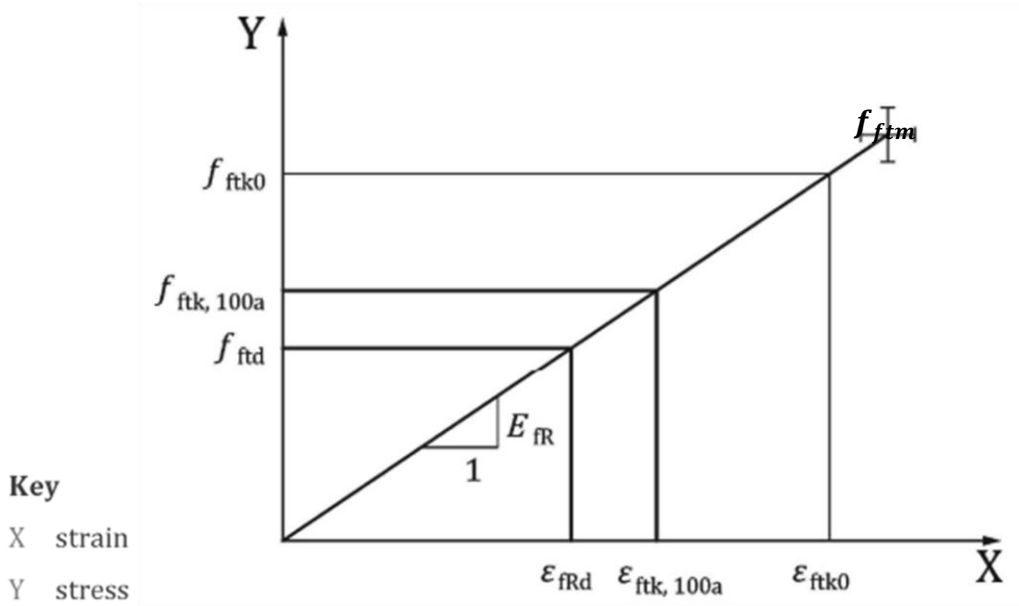


***Figure 4.4:*** *Design stress-strain-diagram for FRP Reinforcement [21]*

***Table 4.3*** *Values of $k_n$ for the 5% characteristic Value according to prEN 1990:2020 [20] Table D.1*

| n | 1 | 2 | 3 | 4 | 5 | 6 | 8 | 10 | 20 |
|---|---|---|---|---|---|---|---|---|---|
| $V_x$ known | 2.31 | 2.01 | 1.89 | 1.83 | 1.80 | 1.77 | 1.74 | 1.72 | 1.68 |
| $V_x$ unknown | - | - | 3.37 | 2.63 | 2.33 | 2.18 | 2.00 | 1.92 | 1.76 |

$V_x$ : Coefficient of variation of a material or product property.

**GFRP Design Material Properties CNR-DT 203/2006**[17]

The following formulas can be used to determine the GFRP Design properties:

$$f_f = E_f \varepsilon_f \tag{4.6}$$

$$\varepsilon_{fd} = 0.9 \cdot \eta \left(\frac{\varepsilon_{fk}}{\gamma_f}\right) \tag{4.7}$$

Where the coefficient (0.9) accounts for the lower ultimate strain of specimens subjected to flexure as compared to specimens subjected to standard tensile tests.

$$\eta = \eta_a \cdot \eta_l \tag{4.8}$$

Where

$f_f$ : FRP Tensile Strength.

$E_f$ : FRP Modulus of Elasticity.

$\varepsilon_f$ : FRP Tensile Strain.

$\varepsilon_{fd}$: Design ultimate FRP tensile strain.

$\varepsilon_{fk}$: Characteristic ultimate FRP tensile Strain.

$\gamma_f$ : Material partial factor. $\gamma_f = 1.5\ (ULS), \gamma_f = 1\ (SLS)$.

$\eta$ : Conversion factor.

$\eta_a$ : Environmental conversion factor. $\eta_a = 0.7\ (ULS, SLS)$.

$\eta_l$ : Conversion factor for long-term effects. $\eta_l = 1(ULS), \eta_l = 0.3(SLS)$.

For ultimate states, the partial factor $\gamma_m$ for FRP bars, denoted by $\gamma_f$, shall be set equal to 1.5. For serviceability limit states, the value to be assigned to the partial factor is $\gamma_f = 1$.

***Table 4.4*** *Environmental conversion factor $\eta_a$ for different exposure conditions of the structure and different fiber types CNR-DT 203/2006*

| Exposure conditions | Type of fiber/ Matrix | $\eta_a$ |
|---|---|---|
| Concrete not-exposed to moisture | Carbon/ Vinylester or epoxy | 1.0 |
| | Glass/ Vinylester or epoxy | 0.8 |
| | Aramid/ Vinylester or epoxy | 0.9 |
| Concrete exposed to moisture | Carbon/ Vinylester or epoxy | 0.9 |
| | Glass/ Vinylester or epoxy | 0.7 |
| | Aramid/ Vinylester or epoxy | 0.8 |

***Table 4.5*** *Conversion factor for long-term effects $\eta_l$ for different types of FRP CNR-DT 203/2006*

| Loading mode | Type of fiber/ Matrix | $\eta_l(SLS)$ | $\eta_l(ULS)$ |
|---|---|---|---|
| Quasi-permanent and/ or cyclic (creep, relaxation and fatigue) | Glass/ Vinylesters or epoxy | 0.30 | 1.00 |
| | Aramid/ Vinylesters or epoxy | 0.50 | 1.00 |
| | Carbon/ Vinylesters or epoxy | 0.90 | 1.00 |

***Table 4.6*** *FRP Design Material Properties*

| $f_{ftk,0}[MPa]$ | $E_f[MPa]$ | $\varepsilon_{fk}$ | $\eta$ | | $\varepsilon_{fd}$ | | $f_{fd}[MPa]$ | |
|---|---|---|---|---|---|---|---|---|
| 984.5 | 55085 | 0.0179 | ULS | SLS | ULS | SLS | ULS | SLS |
| | | | 0.7 | 0.21 | 0.0075 | 0.0034 | 413.5 | 186.1 |

### *4.2.2. Minimum GFRP Reinforcement*

According to **CNR-DT 203/2006**[17] the concrete cover $d_s$ shall be determined as recommended in the current building code for traditional steel reinforced concrete structures. In addition, $d_s$ shall satisfy the following limitations:

$$d_s \geq \begin{cases} 25\ mm\ (two - ways\ slabs) \\ 30\ mm\ (one - ways\ slabs) \\ 35\ mm\ (colimns) \end{cases}$$

$$d_s = d_b + 10 \qquad (4.9)$$

$$using\ GFRP\ rebars\ \phi 12\ mm \therefore d_s = 12 + 10 = 22\ mm\ < 30\ mm$$

$$\therefore d_s = 30\ mm$$

$$d = h - d_s - \frac{d_b}{2} \qquad (4.10)$$

$$\therefore \mathrm{d} = 170 - 30 - \frac{12}{2} = 134\ mm$$

Where

$d_s$: Concrete Cover.

$d_b$: GFRP Rebar Diameter.

d : Effective Depth.

h : Concrete Cross Section Height.

***Table 4.7*** *Bridge Edge Curb Geometry proposed from the company*

| BEC Section Geometry [mm] | | |
|---|---|---|
| Width (b) | 700 | 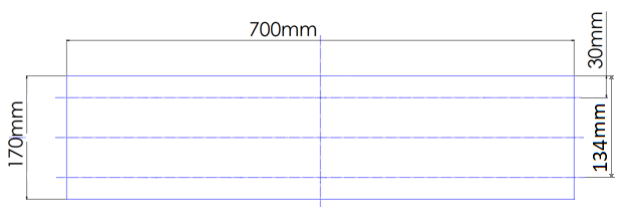  |
| Height (h) | 170 | |
| Concrete Cover ($d_s$) | 30 | |
| Effective Depth (d) | 134 | |

**Direct calculations for the Min. GFRP reinforcement according to CNR-DT 203/2006**[17]

The amount of longitudinal FRP reinforcement in tension shall not be less than the minimum value that satisfies the following equation:

$$M_{Rd} = 1.5 \cdot M_{cr} \tag{4.11}$$

Where $M_{cr}$ is the cracking moment to be determined according to the current building code.

For elements that do not require shear reinforcement, $\rho_f = A_f/(b \cdot d) \geq 0.01$

The calculations for the Cracking Moment $M_{cr}$ was performed as following according to **Cosenza et al.** [22]:

$$M_{cr} = \frac{\sigma_t \cdot I}{n'(h-x)} \tag{4.12}$$

$$\sigma_t = \frac{f_{ctm}}{1.2} \tag{4.13}$$

$$I = \frac{bx^3}{3} + nA_{tot.sup}(x-c)^2 + nA_{tot.inf}(b-x)^2 + n'\frac{b(h-x)^3}{3} \tag{4.14}$$

$$n = \frac{E_f}{E_c} \tag{4.15}$$

$$x = \frac{\frac{bh^2}{2} + n(A_{tot.sup} \cdot C + A_{tot.inf} \cdot d)}{bh + n(A_{tot.sup} + A_{tot.inf})} \tag{4.16}$$

Where

$M_{cr}$ : Cracking Moment [N.mm].

$\sigma_t$ : normal tensile stress in the most stressed fiber [MPa].

I : Moment of Inertia [mm$^4$].

$n'$ : Ratio between Young's Modulus in compression, and tension zones in concrete ($n' = 1$).

x : Position of The Neutral Axis Depth [mm].

$f_{ctm}$ : Mean value of axial tensile strength of concrete.

b : Concrete Cross Section Width [mm].

$h$ : Concrete Cross Section Height [mm].

$n$ : Relationship between the elastic modulus of the FRP bar and concrete.

$E_f$ : Modulus of Elasticity of FRP bar.

$E_c$ : Modulus of Elasticity of Concrete.

$c$ : Concrete Cover [mm].

$A_{tot.sup}$: Area of FRP bars in Compression [mm$^2$].

$A_{tot.inf}$ : Area of FRP bars in Tension [mm$^2$].

The following equation was used to calculate the moment capacity:

$$M_{Rdb} = A_f f_{fd} z \quad (4.17)$$

$$z = d - 0.4x = \left(1 - 0.4\frac{\varepsilon_{cu}}{\varepsilon_{fd}+\varepsilon_{cu}}\right)d \quad (4.18)$$

Where

$\rho_f$ : Reinforcement Ratio.

$b$ : Concrete Cross Section Width [mm].

$M_{Rdb}$: Moment Capacity [N.mm].

$A_f$ : Cross-Sectional Area of GFRP Rebars Reinforcements [mm$^2$].

$f_{fd}$ : Design Tensile Strength of FRP [MPa].

z : Lever arm of internal forces [mm].

x : Neutral axis depth [mm].

$\varepsilon_{cu}$ : Ultimate Concrete Compressive Strain.

$\varepsilon_{fd}$ : Design Tensile Strain of FRP.

**Calculations for the Min. GFRP reinforcement based on Flexural failure modes according to CNR-DT 203/2006**[17]

Flexural failure takes a place when:

- Ultimate concrete compressive strain, $\varepsilon_{cu}$ is reached (Concrete Crushing).
- Design maximum FRP tensile strain, $\varepsilon_{fd}$ is reached (FRP Failure).

The reinforcement ratio $\rho_f$, and the balanced reinforcement ratio $\rho_{fb}$ are required to define the failure mode.

$$\rho_f = \frac{A_f}{bd} \quad (4.19)$$

$$\rho_{fb} = \eta\lambda\frac{f_{cd}}{f_{fd}}\frac{E_f\varepsilon_{cu}}{E_f\varepsilon_{cu}+f_{fd}} \quad ,where\ (EC2: \eta = 1, \lambda = 0.8) \quad (4.20)$$

If $\rho_f < \rho_{fb}$ $(f_f = f_{fb}, \varepsilon_c < \varepsilon_{cu})$ $\quad then$ $\boldsymbol{FRP\ Rupture.}$

The moment capacity for FRP rupture:

$$M_u = \rho_f f_{fd}\left(1 - 0.5\frac{\rho_f f_{fd}}{f_{cd}}\right)bd^2 \quad (4.21)$$

If $\rho_f > \rho_{fb}$ $(f_f < f_{fb}, \varepsilon_c = \varepsilon_{cu})$ $\quad then$ $\boldsymbol{Concrete\ Crushing.}$

The moment capacity for Concrete Crushing:

$$M_u = \rho_f f_f \left(1 - 0.5\frac{\rho_f f_f}{f_{cd}}\right) bd^2 \qquad (4.22)$$

$$f_f = \left(\sqrt{\frac{(E_f \varepsilon_{cu})^2}{4} + \frac{0.8 f_{cd}}{\rho_f} E_f \varepsilon_{cu}} - 0.5 E_f \varepsilon_{cu}\right) \leq f_{fd} \qquad (4.23)$$

Using iterative method according to the previous mentioned procedures, we found that the minimum area of reinforcements required in tension sides is:

$$A_{tot,inf} = 452.39\ mm^2$$

So, with the proposed $GFRP\ rebars\ \phi 12\ mm$, the minimum number of GFRP rebars required are 4 rebars in tension side, and will use the minimum number of 2 GFRP rebars in compression side required for positioning the transverse reinforcements in the right place.

### *4.2.3. Flexural Capacity*

Certainly, with anchors placed every 0.5 meters along the bridge edge curb, the BEC can effectively be treated as a simply supported beam. This configuration allows for more precise analysis and design considerations, as it accounts for the support provided by the anchors at regular intervals, ensuring the stability and load-bearing capacity of the curb during and after the proposed intervention with GFRP reinforcements.

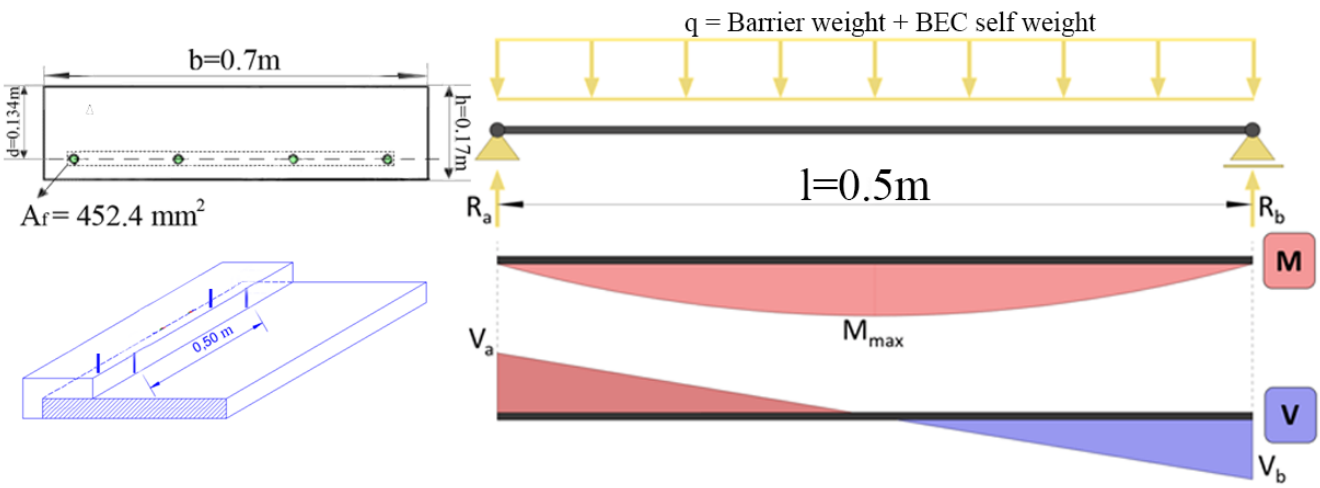


***Figure 4.5:*** *load scheme*

## Load Combination:

The weight of the barrier per unite length

$$W_{barr.} = 3\ [kN/m]$$

BEC self-wight per unite length

$$W_{BEC.} = (0.17 * 0.7)[m^2] * 25\ [kN/m^3] = 2.975\ \cong 3\ [kN/m]$$

Both loads are permanent and unfavorable load

$$\therefore q = \sum \gamma_G \cdot G_k = 1.5\ (3 + 3) = 9\ [kN/m] \qquad (4.24)$$

BEC considered as simply supported beam

$$M_{Ed.} = \frac{ql^2}{8} = 0.28 \cong 0.3\ [kN.m] \qquad (4.25)$$

BEC Resistant moment capacity as mentioned before **Equation (4.17)**

$$M_{Rdb} = A_f f_{fd} z$$

$$M_{Rdb} = 452.4 * 413.5 * 117 = 21886885.8\ [N.mm]$$

$$\therefore (\boldsymbol{M_{Rdb.}} = \mathbf{21.89}\ [\boldsymbol{kN.m}]) > (\boldsymbol{M_{Ed.}} = \mathbf{0.3}\ [\boldsymbol{kN.m}])\ \checkmark$$

Then, the flexural capacity is satisfied.

### *4.2.4. Shear Design*

According to **CNR-DT 203/2006** [17]:

BEC considered as simply supported beam

$$V_{Ed.} = \frac{ql}{2} = 2.25\ [kN] \qquad (4.26)$$

BEC Resistant shear capacity

1- Shear capacity for BEC without shear reinforcements

$$V_{Rd.} = min.\ (V_{Rd,ct.}\ , V_{Rd,max.}) \qquad (4.27)$$

Where

$V_{Rd,ct.}$ : Concrete contribution to the shear strength.

$V_{Rd,max.}$ : Maximum strength of the compressed strut (EC2:2004)[19].

$V_{Rd,ct.}$ Can be computed as follows:

$$V_{Rd,ct.} = 1.3 \cdot \left(\frac{E_f}{E_s}\right)^{0.5} \cdot \tau_{Rd} \cdot k \cdot (1.2 + 40\rho_l) \cdot bd \qquad (4.28)$$

Satisfying the limitation $1.3 \cdot \left(\frac{E_f}{E_s}\right)^{0.5} \leq 1$

Where

$E_f$ *and* $E_s$ : Represents the Young's moduli of elasticity of FRP and steer bars [N/mm$^2$] respectively.

$\tau_{Rd}$ : The design shear stress [N/mm$^2$], defined as: $\tau_{Rd} = 0.25 \cdot f_{ctd} = 0.25 \cdot \frac{0.7 f_{ctm}}{\gamma_c}$

$k = 1$ if more than 50% of the bottom reinforcement is interrupted, otherwise $k = (1.6 - d) \geq 1$, while d in [m]

$\rho_l = \frac{A_f}{b \cdot d}$ which should not be assumed to be larger than 0.02

$$\therefore \boldsymbol{V_{Rd,ct.} = 42.2\ [kN]}$$

$V_{Rd,max.}$ Can be computed as follows:

$$V_{Rd,max.} = \alpha_{cw} \cdot b_w \cdot Z \cdot \nu_1 \cdot f_{cd} \left(\frac{1}{cot(\theta) + tan(\theta)}\right) \qquad (4.29)$$

Where

$\alpha_{cw} = 1$ for non-prestressed structures.

$Z = 0.9 \cdot \mathrm{d}$

$\nu_1 = 0.6 \cdot \left[1 - \frac{f_{ck}}{250}\right]$

The angle $\theta$ should be limited as 1 ≤ cot $\theta$ ≤ 2.5, assume $\theta$=45˚

$$\therefore \boldsymbol{V_{Rd,max.} = 357\ [kN]}$$

Then $$\boldsymbol{V_{Rd,ct.} < V_{Rd,max.}}$$

$$\therefore \boldsymbol{V_{Rd.} = V_{Rd,ct.} = 42.2\ [kN]}$$

$$\therefore (\boldsymbol{V_{Rd.} = 42.2\ [kN]}) > (\boldsymbol{V_{Ed.} = 2.25\ [kN]})\ \checkmark$$

Then, the shear capacity is satisfied.

So, No need for shear reinforcements but we will use the minimum number of stirrups in order to maintain the longitudinal reinforcements in place.

2- The minimum area of shear reinforcement shall be computed as follows:

$$\frac{A_{fw,min.}}{s} = 0.06 \cdot \sqrt{f_{ck}} \cdot \frac{b}{0.004 \cdot E_f} \geq \frac{0.35 \cdot b}{0.004 \cdot E_f} \qquad (4.30)$$

Where

$A_{fw,min.}$: is the area of shear reinforcement.

Also, FRP reinforced concrete beams shall have at least three stirrups per meter and in no case shall be $s \geq 0.8 \cdot d$

$$\therefore \frac{A_{fw,min.}}{s} = 0.93 \geq 1.021$$

$$\frac{A_{fw,min.}}{s} = 1.021\, mm^2/mm$$

$\therefore Considering$ that 8$mm\ diameter\ GFRP\ bar\ gives\ A_{fw.}$ 100.5 $mm^2$ (2 $legs\ per\ stirrup$), $which\ means\ that\ the\ maximum\ spacing\ of$ 99 $mm$ is required. Therefore the proposed shear reinforcement will consist of **Ø8/90 mm**

### *4.2.5. Service Limit State*

SLS - Service Limit State design concepts:

- Deflection Control.
- Cracking Control.
- Stress Limitation.

Bothe deformations and deflections do not attain excessive values, so as to inhibit the normal use of structure, induce damage to non-supporting elements, and cause psychological disturbances to the users.

The stress level in all materials in properly limited in order to avoid FRP bars rupture under continuous stress as well as to mitigate creep phenomena in the concrete.

Cracking phenomena are properly limited to not significantly affect the durability of the structures, their functionality, their aspects, and damage the integrity of the adhesive bond at the FRP – Concrete interface.

#### 4.2.5.1. Deflection Control

According to **CNR-DT 203/2006** [17] the adopted deflection model shall take into account the following:

- Appropriate concrete Young's modulus of elasticity depending upon concrete curing at the time of loading.
- Creep and shrinkage of concrete.
- Concrete stiffening between cracks.
- Thermal loads.
- Static and/or dynamic loads.
- Deflection computation for FRP reinforced members can be performed by integration of the curvature diagram. Such diagram can be computed with non-linear analyses by taking into account both cracking and tension stiffening of concrete.
- Alternatively, simplified analyses are possible, similar to those used for traditional RC members.

Experimental tests have shown that the model proposed by Eurocode2 (EC2) when using traditional reinforced concrete members can be deemed suitable for FRP reinforced concrete elements too. Therefore, the following EC2 equation to compute the deflection $f$ can be considered:

$$f = f_1\beta_1\beta_2\left(\frac{M_{cr}}{M_{max.}}\right)^m + f_2\left[1 - \beta_1\beta_2\left(\frac{M_{cr}}{M_{max}}\right)^m\right] \qquad (4.31)$$

Where

$f_1$ : The deflection of the uncracked section.

$f_2$ : The deflection of the cracked section.

$\beta_1$=0.5: is non-dimensional coefficient accounting for bod properties of FRP bars.

$\beta_2$ : is non-dimensional coefficient accounting for the duration of loading (1.0 for short term loads, 0.5 for long time or cyclic loads).

$M_{max.}$ : The maximum moment acting on the examined element.

$M_{cr}$ : The cracking moment calculated at the same cross section of max. M.

$m$ : A coefficient to be set equal to 2.

## Cracked beam deflection

$$\boldsymbol{n_f = \frac{E_{FRP}}{E_c} = 1.7}$$

$$\boldsymbol{S_n = 0}$$

$$\boldsymbol{\frac{bx^2}{2} - b\frac{(h-x)^2}{2} - n_f A_f (d-x) = 0}$$

$$\boldsymbol{\therefore x = 85.3\ [mm]}$$

$$\boldsymbol{I_{n,gross} = \frac{bx^3}{3} + b\frac{(h-x)^3}{3} + n_f A_f (d-x)^2 = 288426396\ [mm^4]}$$

**According to NTC 2018** [23]

The average value of the tensile strength due to bending is assumed, in the absence of direct experimentation, equal to:

$$f_{ctm,fl} = 1.2\ f_{ctm}$$

$$M_{cr} = \frac{f_{ctm,fl}\, I_{n,gross}}{(h-x)} = 11.3\ [\mathrm{kN.m}]$$

$$f_1 = \frac{5ql^4}{384E_c I_{n,gross}} = 7.86 * 10^{-4}\ [mm]$$

## Uncracked beam deflection

$$\boldsymbol{n_f = \frac{E_{FRP}}{E_c} = 1.7}$$

$$\boldsymbol{S_n = 0}$$

$$\boldsymbol{\frac{bx^2}{2} - n_f A_f (d-x) = 0}$$

$$\boldsymbol{\therefore x = 16.1\ [mm]}$$

$$\boldsymbol{I_{n,cr} = \frac{bx^3}{3} + n_f A_f (d-x)^2 = 11664292.89\ [mm^4]}$$

$$f_2 = \frac{5ql^4}{384E_c I_{n,cr}} = 0.019\ [mm]$$

## Beam deflection

$$f = f_1\beta_1\beta_2\left(\frac{M_{cr}}{M_{max.}}\right)^m + f_2\left[1 - \beta_1\beta_2\left(\frac{M_{cr}}{M_{max}}\right)^m\right]$$

Satisfying $$\left[1 - \beta_1\beta_2\left(\frac{M_{cr}}{M_{max}}\right)^m\right] \geq 0$$

$$\boldsymbol{\therefore f = 0.28\ mm}$$

#### 4.2.5.2. Cracking Control

According to **CNR-DT 203/2006** [17], it's recommended to consider only permanent loading for crack control. Under no circumstances crack width of FRP reinforced structures shall be higher than 0.5 mm.

Experimental tests in FRP reinforced members (with the exception of smooth bars) showed the suitability of the relationships provided by the EC2 for computation of both distance between cracks and concrete stiffening.

The following equation can be used:

$$w_k = \beta s_m \varepsilon_{fm} \tag{4.32}$$

Where

$w_k$: The characteristic crack width, in [mm].

$\beta$ : Coefficient relating average crack width to the characteristic value, to be set equal to q.7 for cracking due to loads.

$s_m$ : The final average distance between cracks, in [mm].

$\varepsilon_{fm}$: The average strain accounting for tension stiffening, shrinkage, etc.

The final average distance between cracks can be computed using the following equation:

$$s_m = 50 + 0.25 \cdot k_1 \cdot k_2 \cdot \frac{d_b}{\rho_r} \tag{4.33}$$

Where

$k_1$: Coefficient accounting for the bond properties of FRP bars, to be equal to 1.6

$k_2$: Coefficient depending upon the strain diagram (0.5 for flexural, 1.0 for pure tension).

$d_b$: The equivalent diameter of the FRP bars, in [mm]; if bars of different diameter are used, their average value can be considered.

$\rho_r$ : The effective reinforcement ratio, equal to $A_f/A_{c,eff}$, where $A_{c,eff}$ is the effective area in tension defined as the concrete area surrounding the tensile

FRP reinforcement, having depth equal to 2.5 times the distance between tension fiber and bars centroid (EC2).

$$A_{c,eff} = 2.5(h-d)\cdot b$$

$$\boldsymbol{s_m = 384.22\ [\mathrm{mm}]}$$

The average strain can be computed using the following equation:

$$\varepsilon_{fm} = \frac{\sigma_f}{E_f}\cdot\left[1-\beta_1\beta_2\left(\frac{\sigma_{fr}}{\sigma_f}\right)^m\right] \qquad (4.34)$$

Satisfying $$\left[1-\beta_1\beta_2\left(\frac{\sigma_{fr}}{\sigma_f}\right)^m\right] \geq 0$$

Where

$\sigma_f$ : The reinforcement stress in tension of the cracked cross section.

$\sigma_{fr}$: The reinforcement stress in tension of the cracked cross section when the first crack is observed.

$m$ : Coefficient to be set equal to 2.

$\beta_1$ *and* $\beta_2$ are coefficients defined in section 4.2.5 (deflection control).

For long term

$$\boldsymbol{n_f = \frac{E_{FRP}}{E_c}\cdot 2 = 3.4}$$

$$\boldsymbol{S_n = 0}$$

$$\boldsymbol{\frac{bx^2}{2} - n_f A_f (d-x) = 0}$$

$$\boldsymbol{\therefore x = 22.17\ [mm]}$$

$$\boldsymbol{I_n = \frac{bx^3}{3} + n_f A_f (d-x)^2 = 21778725.9\ [mm^4]}$$

$$\boldsymbol{\sigma_f = \frac{M}{I_n}(d-x)n_f = 5.24\ [MPa]}$$

$$\boldsymbol{\sigma_{fr} = \frac{M_{cr}}{I_n}(d-x)n_f = 197.3\ [MPa]}$$

$$\varepsilon_{fm} = 0\ mm$$

$$\therefore w_k = \beta s_m \varepsilon_{fm} = 0\ mm\ \checkmark$$

The crack width check is satisfied.

#### 4.2.5.3. Stress Limitation

According to **CNR-DT 203/2006** [17], the design hypotheses are as follows:

- Linear elastic behaviour of materials.
- Plane cross-beam sections before loading remains plane after loading.
- Perfect bond exists between the concrete and FRP bars.

The stress in the FRP reinforcement at SLS under the quasi-permanent load shall satisfy the limitation $\sigma_f \leq f_{fd}$, $f_{fd}$ being the FRP design stress at SLS.

For long term

$$n_f = \frac{E_{FRP}}{E_c} \cdot 2 = 3.4$$

$$S_n = 0$$

$$\frac{bx^2}{2} - n_f A_f (d - x) = 0$$

$$\therefore x = 22.17\ [mm]$$

$$I_n = \frac{bx^3}{3} + n_f A_f (d - x)^2 = 21778725.9\ [mm^4]$$

$$\sigma_c = \frac{M}{I_n} x = 0.31\ [MPa]$$

$$\sigma_f = \frac{M_c}{I_n} (d - x) n_f = 5.24\ [MPa]$$

$$\therefore\ \sigma_f = 5.24\ [MPa] < f_{fd} = 186.1\ [MPa]\ \checkmark$$

The stress limitation check is satisfied.

### *4.2.6. Impact Stability Check*

This section encompasses a pivotal impact stability check for the bridge edge curb (BEC), a critical examination that holds substantial importance in ensuring overall stability. This check is of paramount significance as it directly assesses the BEC's ability to maintain stability, particularly during potential vehicle crashes. The successful fulfilment of this stability check is instrumental in bolstering the effectiveness of the bridge barrier, thus attaining a heightened level of safety for both the bridge structure and its occupants. By rigorously evaluating the BEC's capability to withstand vehicle impacts, this check contributes significantly to the assurance of structural integrity and the safeguarding of individuals traveling on the bridge.

Initiating the impact stability check necessitates a comprehensive understanding of the various actions and loads exerted upon the Bridge Edge Curb (BEC). This preliminary step serves as the foundation for a rigorous analysis, ensuring a comprehensive assessment of the BEC's stability under various scenarios. By discerning the range of forces and loads at play, including those arising from vehicle impacts, dynamic loads, and external forces, engineers can accurately model and predict the BEC's response to different conditions. This holistic comprehension of the BEC's load-bearing capacity is instrumental in driving a reliable impact stability check, a pivotal procedure aimed at validating the structural robustness of the BEC and its capacity to withstand critical situations.

According to NTC [23], In the absence of specific requirements, the forces caused by accidental collisions on the safety elements can be taken into account in the structural design of bridges through an equivalent horizontal collision force of 100 kN. It represents the effect of the impact to be transmitted to the restraints and shall be considered to act transversely and horizontally 100mm below the top of the element or 1.0m above the level of the roadway, whichever is smaller.

Schemes commonly used in curb design use the following definition of the system of forces equivalent to the actions caused by collisions on safety elements under ordinary design conditions [4]:

- **Transversal forces**: four horizontal forces are assumed in correspondence with the uprights of the barrier, whose center distance is established at 1.25 m; the two forces applied to the end posts of the considered area are equal to 50kN and the other two, applied to the internal

uprights, are equal to 100kN. All forces act transversely at a height of 1.00 m from the road surface and are directed towards the outside of the deck;

- **Vertical loads**: in addition to the structure's own weight (Barrier weight which can be assumed to be equal to 3 kN/m, and the BEC weight), the Load Scheme 2 envisaged in the NTC [23] is considered **(Figure 4.7)**, consisting of two load imprints of dimensions 0.35 x 0.60 m on each of which a force of 200 kN is applied; the footprints are placed longitudinally in the middle of the deck area affected by the application of the aforementioned horizontal load and transversally one is placed at the end of the road platform while the other is 2.00 m away from it; The equivalent load scheme described above can be represented as shown in the following **Figure 4.6**.

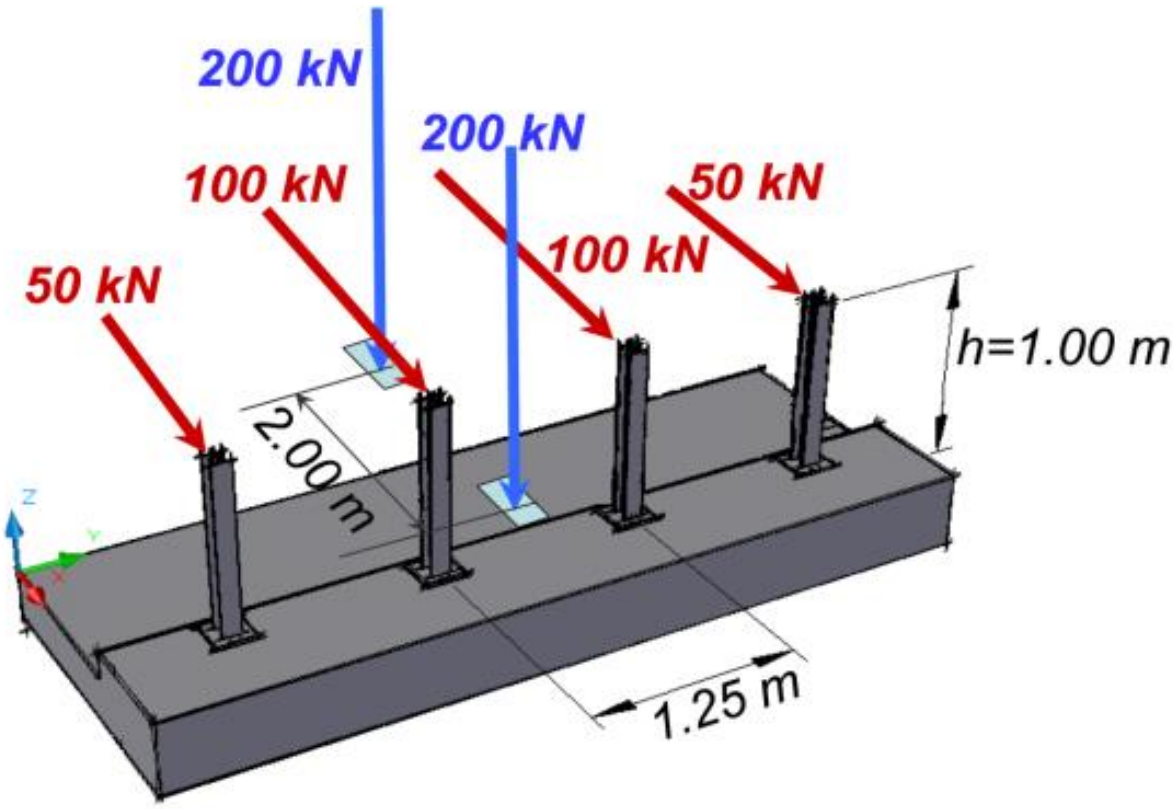


***Figure 4.6:*** *Global load scheme to be considered in the case of "ordinary" design conditions (the representation of th e permanent loads is omitted) [4]*

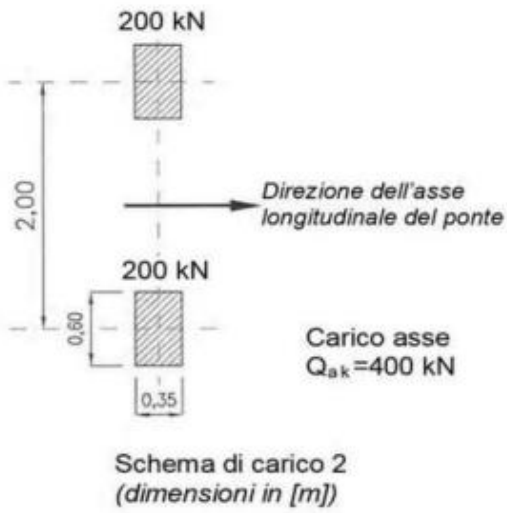


***Figure 4.7:*** *Load diagrams 1 – 5 (dimensions in m) NTC [23]*

In the context of the impact stability check for the Bridge Edge Curb (BEC), the evaluation encompasses a set of critical forces. A singular horizontal force signifies the impact exerted by vehicular collision against the bridge barrier. Concurrently, three distinct vertical forces are at play, encompassing the barrier's weight, the BEC's weight, and one of two load imprints with dimensions 0.35 x 0.60 m, carrying a force of 200 kN. **(Figure 4.7)**

These forces engender both stability and instability influences within the structure. Stability forces generate moments that contribute to the structure's steadfastness, maintaining its positional equilibrium. Conversely, instability forces generate moments that act in opposition to the structure's stability, potentially causing instability. Notably, within this scenario, the three vertical loads—the barrier weight, the BEC weight, and the load imprint—are identified as stability loads. In contrast, the horizontal force represents an instability force.

A pivotal criterion in this analysis stipulates that the cumulative impact of stability loads should surpass that of instability loads.

$$\boldsymbol{M_{Stab.}} > \boldsymbol{M_{Inst.}}$$

This requirement underscores the necessity for the BEC to exhibit a robust resistance against potential instabilities, with stability forces outweighing their instability counterparts. This meticulous evaluation ensures that the BEC is well-equipped to withstand dynamic conditions, reaffirming its role in fortifying the overall structural stability of the bridge and promoting the safety of its occupants.

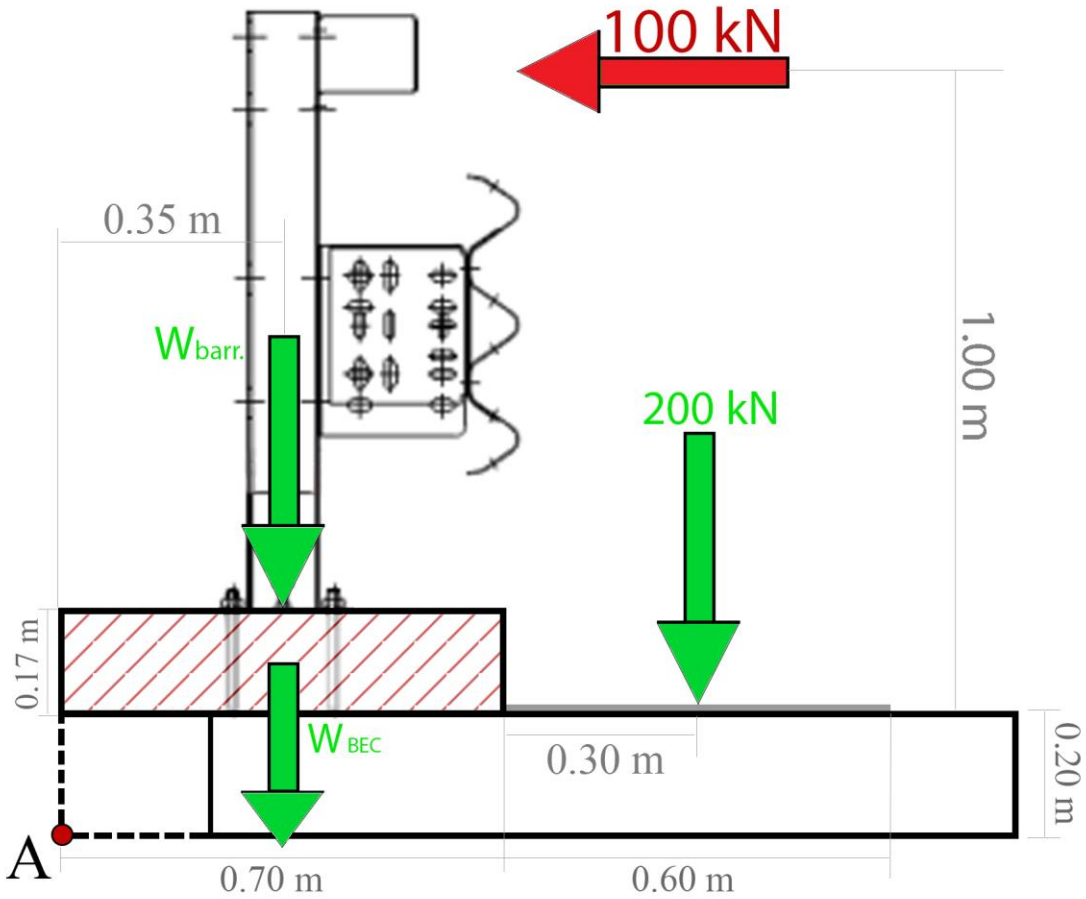


*Figure 4.8: 2-D Load Diagram For impact stability Check*

All the Moments will be calculated around point (A) which represents the most affected part due to it has the longest moment arm.

**Instability moment calculations:**

$$M_{Inst.} = 100\ [kN] * (1 + 0.2)[m] = \mathbf{120\ kN.m}$$

**Stability moment calculations:**

The weight of the barrier

$$W_{barr.} = 3\ [kN/m] * 1\ [m] = 3kN$$

The weight of the BEC

$$W_{BEC.} = Volume\ per\ unite\ length * density$$
$$= (0.17 * 0.7 * 1)[m^3] * 25\ [kN/m^3] = 2.975\ kN$$

Then

$$M_{Stab.} = (3\ [kN] * 0.35\ [m]) + (2.975\ [kN] * 0.35\ [m]) + (200[kN] * (o.3 + 0.7)[m])$$

$$M_{Stab.} = \mathbf{202.1\ kN.m}$$

$$\therefore \boldsymbol{M_{Stab.}} > \boldsymbol{M_{Inst.}} \checkmark$$

# 5. CONCLUSIONS AND FUTURE SCOPE

This thesis embarks on an extensive exploration of the Bridge Edge Curb (BEC), a critical component of bridge infrastructure, to study the feasibility of replacing the steel reinforcements with Glass Fiber Reinforced Polymer (GFRP) reinforcements.

The journey commences with a meticulous definition of the BEC, followed by an incisive examination of its defects through an empirical statistical analysis of inspection data garnered from a diverse array of bridges. This meticulous investigation uncovers a recurrent culprit—corrosion in steel reinforcement rebars—as the predominant catalyst behind these defects. Drawing from these insights, the implementation of GFRP rebars emerges as an efficacious antidote to this corrosion-related degradation. This corrosion-resistant alternative presents immense potential for mitigating deterioration, thereby enhancing the longevity and safety of pivotal bridge elements.

Central to this thesis is the consequential experimental campaign dedicated to GFRP rebars characterization, where their tensile strength is pivotal. As a linchpin in structural design, this property elucidates the maximum axial load a material can bear until failure. Given its pronounced influence on structural integrity, the tensile strength of GFRP rebars holds pivotal significance. This campaign's application in BEC reinforcement necessitates an accurate determination of this parameter according to CNR-DT 203/2006 and ISO 10406-1:2008 to facilitate their optimal integration within specified design parameters.

Subsequently, the thesis delves into the design and verification of the BEC, meticulously adhering to codes and standards (CNR-DT 203/2006, EN 1992-1-1:2004, and prEN 1990). The minimum GFRP reinforcements, tailored to the proposed geometry and compatible with the designated barrier, are defined, comprising six bars strategically positioned for optimal reinforcement: four bars on the tensioned side and two bars on the compressive side. Moreover, a paramount focus rests on the verification of impact stability checks, a critical determinant of the BEC's capacity to maintain equilibrium, especially during potential vehicular impacts. The successful completion of this assessment augments the bridge barrier's efficiency, thereby elevating both the structure's safety and the well-being of its occupants.

As the thesis seamlessly threads through these facets, it culminates in a comprehensive contribution to the field of bridge engineering, spotlighting the potential of GFRP as a transformative solution for enhancing the durability, safety, and resilience of critical transportation infrastructure.

Certainly, the transition from steel rebars to (GFRP) rebars in the design of the Bridge Edge Curb (BEC) necessitates a critical step: the certification of GFRP materials. Certification is vital to ensure that the GFRP rebars meet the required mechanical properties and standards for structural applications.

To achieve this, an experimental campaign is essential. This campaign involves a series of rigorous laboratory tests and analyses designed to characterize the mechanical properties of GFRP materials. These tests typically include tensile, flexural, shear, and compressive tests, among others. The results of these tests will provide critical data on the strength, stiffness, and other key mechanical characteristics of GFRP rebars.

Once the GFRP rebars pass the certification process and meet the necessary standards, they can be confidently integrated into the BEC design. This certification process is a crucial step in ensuring the safety and reliability of the bridge structure when using innovative materials like GFRP.

The experimental campaign embarked on a journey to characterise the tensile strength of GFRP rebars. While this endeavour was infused with promise, it was not devoid of challenges and limitations, notably the constraint of time. As GFRP rebars were relatively novel in this context, the characterization tests demanded tailored considerations.

The preliminary phase involved test setup preparations, entailing the intricate installation of steel anchors onto the test specimens for subsequent testing. Initially, hollow mild steel pipes were employed, paired with Superfluid two-component epoxy resin for injections and anchoring EPOJET 09 CPR-IT1/0095 to bond the steel tube with the GFRP bars. However, this configuration exhibited limitations, primarily debonding between the epoxy and the mild steel pipe, prompting a shift to more resilient alternatives. Subsequently, self-drilling hollow bars with continuous thread steel pipes were introduced, paired with epoxy resin for structural chemical fixing, Epoxy MAPEFIX EP 100 N.CPR-IT1/0921—a more robust albeit costlier hardener. This alteration yielded improved outcomes, yet instances of debonding persisted.

To address these challenges and enhance the anchorage's performance, several recommendations for future improvement can be made. To begin with, exploring the adoption of an epoxy adhesive with greater strength could significantly enhance the bond between the GFRP bars and steel anchors. While this might entail a higher cost, the potential benefits in terms of improved adhesion and test reliability could outweigh the expenses.

In addition to optimising the bond between the steel tube and the GFRP bars, a strategic approach could involve choosing the inner diameters of the tubes to correspond with the diameters of the bars being tested. By aligning these dimensions, the volume filled with the adhesive can be reduced to a minimum while still maintaining strong adhesion. This reduction in adhesive volume enhances the effectiveness of the bond between the tube and the bar. This approach not only improves the overall bond strength but also conserves the adhesive material, potentially leading to cost savings while ensuring better performance in the experimental campaign.

Furthermore, try another type of steel pipe that might behave better and have good bonding with the adhesive used, e.g., galvanised steel pipe, etc.

To conclude, to mitigate the risk of rejected specimens during preparation or testing, a strategic approach is better—ordering a surplus of bars beyond the actual requirement.

By implementing these recommendations, the potential for debonding between the epoxy and the steel tube could be effectively mitigated. Additionally, this approach takes into consideration both the need for superior adhesive properties and the importance of cost control. Ultimately, these improvements could lead to more reliable and consistent results in the experimental campaign, ensuring the accurate characterization of GFRP rebar tensile strength for its successful integration in structural applications. While these challenges underscored the evolving nature of working with novel materials and the need for meticulous setup preparations, the experimental campaign remained instrumental in furnishing valuable insights into the mechanical behaviour of GFRP rebars, paving the way for their potential applications in bridge engineering.

The utilization of Glass Fiber Reinforced Polymer (GFRP) rebars in the design of the Bridge Edge Curb (BEC) has demonstrated its potential as a promising solution. By replacing traditional steel rebars with GFRP, this innovative approach effectively addresses concerns related to corrosion, significantly enhancing the reliability and durability of Bridge Edge Curbs.

Moreover, the design incorporating GFRP rebars has successfully met the rigorous requirements and checks, including those related to flexural strength, shear capacity, and service limit states such as deflection, cracking width, and stress limitation. This not only underscores the proficiency of the GFRP-based design but also highlights its potential to contribute to safer, more sustainable, and long-lasting infrastructure solutions in the future.

The future scope of this study offers several avenues for further exploration and enhancement. First and foremost, incorporating the insights gained from the challenges faced during the experimental campaign will be crucial. This includes considering the previously mentioned considerations for optimising the setup of the tensile test for GFRP rebars to accurately characterise their tensile capacity. Moreover, extending these considerations to the design of the BEC using GFRP rebars instead of steel will ensure a comprehensive understanding of the material's behaviour in various applications.

To validate the theoretical design calculations for the BEC with GFRP rebars, the implementation of experimental tests on actual BEC structures can provide invaluable verification. Additionally, simulating a vehicle crash onto the bridge barrier to satisfy the impact stability check will contribute to a more comprehensive evaluation of the BEC's performance under real-world scenarios.

Looking ahead, exploring the replacement of steel transverse reinforcements and steel anchors used to connect the BEC with the bridge slab with GFRP stirrups and anchors presents an exciting prospect. This expansion of the study can further enhance the durability and corrosion resistance of critical bridge components, offering a sustainable and resilient alternative. As the field of composite materials continues to advance, these future avenues of investigation hold the potential to revolutionise bridge engineering practices, promoting safer and more sustainable transportation infrastructure.

**Acknowledgements**

I would like to express my sincere gratitude and acknowledgment to ATP Company for their unwavering effort and steadfast commitment throughout the duration of this thesis. Their partnership and support were instrumental in the successful completion of this research, and their dedication to the advancement of engineering solutions has left an indelible mark on this work. ATP Company's contributions have not only enriched my academic journey but have also contributed to the broader field of structural engineering. I am deeply thankful for their trust and collaboration, which have undoubtedly elevated the quality and impact of this thesis.

# REFERENCES


[1] G. Santarsiero, A. Masi, V. Picciano, and A. Digrisolo, “The Italian guidelines on risk classification and management of bridges: Applications and remarks on large scale risk assessments,” *Infrastructures (Basel)*, vol. 6, no. 8, 2021, doi: 10.3390/infrastructures6080111.

[2] O.-A. Tekniikan, J. A. Liikenteen Ala T E K I J Ä :, and L. Vesalo, “SILLAN REUNAPALKIN RAKENNEANALYYSI KAIDETÖRMÄYKSELLE.”

[3] “APPENDICE AL MANUALE DELLA SORVEGLIANZA CATALOGO DIFETTI dicembre 2020 rev.1.”

[4] “I QUADERNI TECNICI Volume II per la salvaguardia delle infrastrutture.”

[5] R. Masmoudi, “Glass fibre reinforced plastic (GFRP) rebars for concrete structures,” 1995.

[6] A. Nanni, “Relevant Field Applications of FRP Composites in Concrete Structures Use of FRCM systems in strengthening applications View project SEACON: Sustainable Concrete Using Seawater View project.” [Online]. Available: https://www.researchgate.net/publication/237703975

[7] C. E. Bakis *et al.*, “Fiber-Reinforced Polymer Composites for Construction-State-of-the-Art Review”, doi: 10.1061/ASCE1090-026820026:273.

[8] A. Zaman, S. A. Gutub, and M. A. Wafa, “A review on FRP composites applications and durability concerns in the construction sector,” *Journal of Reinforced Plastics and Composites*, vol. 32, no. 24. pp. 1966–1988, Dec. 2013. doi: 10.1177/0731684413492868.

[9] E. Gudonis, E. Timinskas, V. Gribniak, G. Kaklauskas, A. K. Arnautov, and V. Tamulėnas, “FRP REINFORCEMENT FOR CONCRETE STRUCTURES: STATE-OF-THE-ART REVIEW OF APPLICATION AND DESIGN,” *Engineering Structures and Technologies*, vol. 5, no. 4, pp. 147–158, May 2014, doi: 10.3846/2029882x.2014.889274.

[10] Z. Wang, X. Zhao, and X. Noori, “State-of-the-art review of FRP composites for major construction with high performance and longevity ‘State-of-the-art review of FRP composites for major construction with high performance and longevity,’” 2014. [Online]. Available: http://en.wikipedia.org/wiki/I-

[11] Y. H. Mugahed Amran, R. Alyousef, R. S. M. Rashid, H. Alabduljabbar, and C. C. Hung, “Properties and applications of FRP in strengthening RC structures: A review,” *Structures*, vol. 16. Elsevier Ltd, pp. 208–238, Nov. 01, 2018. doi: 10.1016/j.istruc.2018.09.008.

[12] X. Zou, H. Lin, P. Feng, Y. Bao, and J. Wang, “A review on FRP-concrete hybrid sections for bridge applications,” *Composite Structures*, vol. 262. Elsevier Ltd, Apr. 15, 2021. doi: 10.1016/j.compstruct.2020.113336.

[13] W. Hu, Y. Li, and H. Yuan, “Review of Experimental Studies on Application of FRP for Strengthening of Bridge Structures,” *Advances in Materials Science and Engineering*, vol. 2020. Hindawi Limited, 2020. doi: 10.1155/2020/8682163.

[14] W. Zhou, P. Feng, and J. Q. Yang, “Advances in coral aggregate concrete and its combination with FRP: A state-of-the-art review,” *Advances in Structural Engineering*, vol. 24, no. 6, pp. 1161–1181, Apr. 2021, doi: 10.1177/1369433220968429.

[15] P. D. Gkournelos, T. C. Triantafillou, and D. A. Bournas, “Seismic upgrading of existing reinforced concrete buildings: A state-of-the-art review,” *Engineering Structures*, vol. 240. Elsevier Ltd, Aug. 01, 2021. doi: 10.1016/j.engstruct.2021.112273.

[16] J. D. Ortiz, S. S. Khedmatgozar Dolati, P. Malla, A. Nanni, and A. Mehrabi, “FRP-Reinforced/Strengthened Concrete: State-of-the-Art Review on Durability and Mechanical Effects,” *Materials*, vol. 16, no. 5. MDPI, Mar. 01, 2023. doi: 10.3390/ma16051990.

[17] “CNR-Advisory Committee on Technical Recommendations for Construction NATIONAL RESEARCH COUNCIL ADVISORY COMMITTEE ON TECHNICAL RECOMMENDATIONS FOR CONSTRUCTION Guide for the Design and Construction of Concrete Structures Reinforced with Fiber-Reinforced Polymer Bars,” 2006.

[18] ISO 10406-1, “Fibre-reinforced polymer (FRP) reinforcement of concrete — Test methods — Part 1: FRP bars and grids,” 2008.

[19] “Eurocode 2: Design of concrete structures-Part 1-1: General rules and rules for buildings,” 2004.

[20] “CEN/TC 250 N 2555,” 2020. [Online]. Available: https://cen.iso.org/livelink/livelink/open/centc250

[21] “EuroCode 2_GFRP internal reinforcement”.

[22] E. Cosenza, G. Manfredi, M. Pecce, and B. Della Progettazione, “HOEPLI STRUTTURE IN CEMENTO ARMATO.”

[23] P. R. T E P R I M A and P. G. Verdi, “GAZZETTA UFFICIALE DELLA REPUBBLICA ITALIANA DIREZIONE E REDAZIONE PRESSO IL MINISTERO DELLA GIUSTIZIA-UFFICIO PUBBLICAZIONE LEGGI E DECRETI-VIA ARENULA, 70-00186 ROMA AMMINISTRAZIONE PRESSO L’ISTITUTO POLIGRAFICO E ZECCA DELLO STATO-VIA SALARIA, 691-00138 ROMA-CENTRALINO 06-85081-LIBRERIA DELLO STATO Aggiornamento delle «Norme tecniche per le costruzioni»,” 2018.